UNIVERSIDADE FEDERAL DE MINAS GERAIS
Instituto de Ciências Exatas
Programa de Pós Graduação em Física

Paulo Fernando Gomes Velloso

A computational probe for molecular environments.

Belo Horizonte
2020

Paulo Fernando Gomes Velloso

A computational probe for molecular environments.

Tese apresentada ao Programa de Pós-Graduação em Física do Instituto de Ciências Exatas da Universidade Federal de Minas Gerais como requisito parcial para obtenção do título de Doutor em Ciências.

Supervisor: José Rachid Mohallem

Belo Horizonte

2020

Dados Internacionais de Catalogação na Publicação (CIP)

V441c Velloso, Paulo Fernando Gomes.
A computational probe for molecular environments / Paulo Fernando Gomes Velloso. – 2020.
97f., enc. : il.

Orientador: José Rachid Mohallem.
Tese (doutorado) – Universidade Federal de Minas Gerais, Departamento de Física.
Bibliografia: f. 75-85.

1. Física molecular. 2. Campo eletrostático. 3. Físico química. 4. Química quântica.
I. Título. II. Mohallem, José Rachid. III. Universidade Federal de Minas Gerais, Departamento de Física.

CDU – 533.7 (043)

Ficha catalográfica elaborada por Romário Martins – CRB6 3595
Biblioteca Professor Manoel Lopes de Siqueira – Departamento de Física - UFMG

Universidade Federal de Minas Gerais
Instituto de Ciências Exatas
Programa de Pós-Graduação em Física
Caixa Postal 702
30.123-970 Belo Horizonte - MG - Brasil

Telefone (xx) (31) 3409 5637
(xx) (31) 3409 5633
Fax (xx) (31) 3409 5688
(xx) (31) 3409 5600
e-mail pgfisica@fisica.ufmg.br

A presente tese, intitulada **"A computational probe for molecular environments"** de autoria de **Paulo Fernando Gomes Velloso** submetida à Comissão Examinadora, abaixo-assinada, foi aprovada para obtenção do grau de **DOUTOR EM CIÊNCIAS**, em vinte de março de dois mil e vinte.

Belo Horizonte, 20 de Março de 2020.

Prof. José Rachid Mohallem
Orientador do estudante
Departamento de Física/UFMG

Prof. Ricardo Wagner Nunes - por videoconferência
Departamento de Física/UFMG

Prof. Jadson Cláudio Belchior
Departamento de Química/UFMG

Prof. André Farias de Moura - por videoconferência
Departamento de Química/UFSCar

Profa. Ginette Jalbert de Castro Faria - por videoconferência
Instituto de Física/UFRJ

Acknowledgements

Agradeço primeiramente à minha esposa, Anne, que me apoiou em todas as minhas escolhas durante esse período. À minha família que sempre investiu nos meus estudos. Aos amigos que me acompanharam. Ao meu orientador pela confiança, e às agências de fomento pelo investimento na minha pesquisa. Agradeço também à CAPES (código 001).

"Nobody exists on purpose, nobody belongs anywhere,
everybody is gonna die. Come watch TV!"
(Morty Smith - Rick and Morty, episode 8: Rixty Minutes)

Resumo

Nessa tese reportamos o uso de uma molécula virtual do tipo HD como sonda para o estudo de ambientes moleculares. A sonda tem momento de dipolo que pode ser ajustado pela modificação das massas nucleares com o uso da FNMC. Ela pode ser usada para fazer análise de ambientes moleculares, em particular, para sondar regiões polarizaveis e para calcular campos eletrostáticos moleculares, os quais são propostos como uma nova métrica para intensidade de ligações intermoleculares. Para testar a sonda, usamos sistemas simples (hidrogênio, água, benzeno e clorobenzeno). Uma vez que a performance da sonda foi comprovada, aplicamos o método para analisar a cavidade de um par de Lewis frustrado, e contribuir para a discussão do mecanismo de ativação da molécula de hidrogênio. Nossos resultados estão de acordo com o modelo de ativação por transferência de elétrons. Além disso, aplicamos o método ao estudo de dois tipos de interações intermoleculares, ligações contendo π- e σ-*hole*. Essas interações são criadas por regiões de potencial eletrostático positivo em moléculas, e são capazes de produzir interações não covalentes com regiões negativas, por exemplo, com pares de elétrons de moléculas contendo nitrogênio ou oxigênio. Baseado no teorema de Hellmann-Feynman, que afirma que ligações intermoleculares são completamente descritas por interações Coulombianas (eletrostática mais polarização), usamos a sonda para calcular os campos elétricos das ligações e usar como um quantificador para as interações.

Palavras-chave: Sonda isotópica, Interações moleculares, Física Molecular, Química Quântica, Campos elétricos moleculares, Potencial elétrico molecular, Pós Born-Oppenheimer, Ambientes Moleculares.

Abstract

In this thesis we report the use of an HD-like virtual molecule used as a probe to study molecular environments. The probe has a dipole moment which is tuned by modifying its nuclear masses using FNMC. It can be used to analyse molecular environments, in particular to probe polarisable molecular regions and to calculate molecular electrostatic fields, which we propose to be used as a new metric of intermolecular bond intensity. To test the probe we used simple systems (hydrogen, water, benzene and chlorobenzene). Once the performance of the probe was assessed, we applied it to analyse the cavity inside a frustrated Lewis pair and contribute to the discussion of the mechanism for hydrogen activation. Our results are in concordance with the electron transfer activation mechanism. We later applied the method to study two types of inter molecular interactions, π- and σ-hole bonds. These interactions are created by regions of positive electrostatic potential in molecules, capable of producing non-covalent interactions with negative regions, for example, lone pairs of molecules containing nitrogen or oxygen. Based on the Hellmann-Feynman theorem, which states that intermolecular bonds are fully described by Coulombian interactions (electrostatic plus polarisation), we used the probe to calculate the electric fields of the bonds and use it as a quantifier for the interactions.

Keywords: Isotopic probe, Molecular Interactions, Molecular Physics, Quantum Chemistry, Molecular Electrostatic Fields, Molecular Electrostatic Potential, Post Born-Oppenheimer, Molecular Environments.

List of Figures

List of Tables

List of abbreviations and acronyms

MEP	Molecular electrostatic potential
BO	Born-Oppenheimer
BOA	Born-Oppenheimer approximation
FNMC	Finite nuclear mass correction
HF	Hartree-Fock
CI	Configurations interaction
DFT	Density functional theory
PES	Potential energy surface
DBOC	Diagonal Born-Oppenheimer correction
UHF	Unrestricted Hartree-Fock
RHF	Restricted Hartree-Fock
ROHF	Restricted Open-shell Hartree-Fock
LATME	Special atoms and molecules laboratory (acronym in portuguese)
FLP	Frustrated Lewis pair
EF	Electric field
TMA	Trymethylamine

Contents

1 Introduction

In this chapter, we will give an overview of what the molecular electrostatic potential is, the ways it can be calculated, how it is used in molecular science and what are the problems concerning its use. We will also present our work, the development of an isotopic probe, able to calculate molecular electrostatic fields, which will be used to quantify interactions and to identify polarisable sites.

In the last decades, *ab initio* methods of quantum chemistry have increased their applicability to the study of structural and spectroscopic properties. However, many important processes in modern science, including the ones involving biological systems, demand a next step, specifically the theoretical knowledge of the properties of molecular environments. This demands the thorough study of the interactions that happen in such environments, and the identification of the reactive sites where each of them happen [1,2]. Molecular electrostatic fields and potentials are considered good auxiliaries to important topics, i.e. identification of reactive sites and the study of hydrogen bonds [3–5], and much of the research done in this area depend on the molecular electrostatic potential (MEP). This observable is, in principle, easy to calculate and, ever since computers had their efficiency increased to perform accurate calculations of electronic structure, it has been used in general to determine electrostatic properties of molecular systems. [6].

The MEP is given by

$$V(\vec{\mathbf{r}}) = \sum_A \frac{Z_A}{|\vec{\mathbf{R}}_A - \vec{\mathbf{r}}|} - \int \frac{\rho(\vec{\mathbf{r}}')\,\mathrm{d}\vec{\mathbf{r}}'}{|\vec{\mathbf{r}}' - \vec{\mathbf{r}}|}, \tag{1.1}$$

in which $\mathrm{Z_A}$ and $\tilde{\mathbf{R}}_\mathrm{A}$ are respectively the charge and position of nucleus A and $\rho(\vec{\mathbf{r}}')$ is the electron density. Its computation is simple and the calculation of the potential in one arbitrary point is very accurate; on the other hand, many points are needed in practical applications, and the computational cost grows with the square of the number of functions used, which is especially costly for large systems [7]. Besides, this calculation depends on the quality of the description of the density $\rho(\vec{\mathbf{r}}')$ [8] and therefore, describing well the electron density is the key to an accurate calculation for the MEP, and the methods used to describe it vary in performance and accuracy. The main one is the point charge method [9–13], which consists in assigning point charge values at the atoms, in a way to replicate the potential that would be obtained by the continuous charge distribution by considering the density simply as the density of point charges plus some distortion caused by the interactions; however, this partitioning of the molecular density into atomic densities is not unique for any molecule [14]. Although there is no physical basis to assigning point charges to atoms, the point charge model is very successful because it is computationally

cheap and easy to implement despite its problems, which include calculations near lone pairs of electrons [15, 16], around atoms of sulphur [17], and anisotropic effects [18].

Other methods that have been proposed to calculate the MEP include: building the potential by molecular fragments [19, 20], using multipolar expansions centered at the nucleus [6, 21–23] or distributed [15, 16, 24, 25], and also the representation of the electron density in terms of spherical harmonic expansions [7, 14, 26, 27]. These methods are a great addition to the field, and they can perform well in their own niche, but we are still missing a more general method to understand what happens when large molecules approach each other, although some attempts were made to try to solve this problem [28–30].

In the study of molecular interactions, the MEP is used as a guide to which regions of the molecule interact with regions of other molecules. Here, the MEP is calculated at the surface of the molecule, a region defined by Bader [31] as the $\rho(\vec{\mathbf{r}}) = 0.01$ a.u. contour surface, which encompasses around 97% of the molecule's electronic charge. Figure 1 shows an example of a molecular electrostatic potential surface, in which the blue indicates more positive potential, and the red indicates more negative potential.

Figure 1 – Example MEPS of $C_6H_3BrF_2$

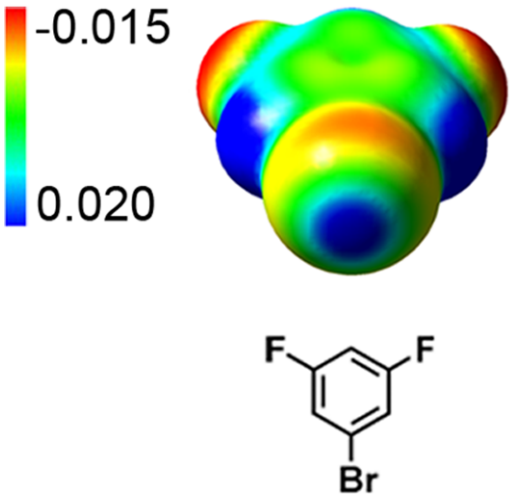

Source – Adapted from reference [32]

This only works under the assumption that the intermolecular interactions are Coulombic (electrostatic plus polarisation) in nature[1] [33–35]. A disadvantage of this kind of surfaces is that predictions based on it, specially for the molecular interactions focused in this work, are mainly based on the molecular potentials of the isolated molecules. As the molecules approach each other two kinds of problems appear. First, MEP surfaces are very

[1] What this means for quantum chemistry is that given an accurate electronic density and geometry, quantum mechanics has no further role in the characterisation of the interactions.

difficult to interpret in the critical region of the very bond; second, further polarisation effects due to the interaction are not taken into account [8, 36].

Important topics like biological recognition [37], hydrogen bonding [38], computer simulations and modelling of molecular complexes and new materials [28, 39, 40], rely on electrical properties of atoms and molecules. And yet, we remain with no general approach to the problem of predicting what happens when large molecules approach each other.

Considering what has been presented, the purpose of this work is to develop a novel way of quantifying intermolecular interactions. This was done by using an isotopic computational probe. The probe is a modified molecule of H_2, with nuclear masses that do not correspond to those of natural hydrogen (or isotopes), and tuned to have a large dipole moment compared to natural isotopologues of H_2. When the symmetry of mass is broken in the probe, there is an isotopic dipole moment, due to the displacement of the electron cloud towards the heavier mass, which cannot be calculated by using traditional Born-Oppenheimer (BO) calculations, because it considers that the nucleus have infinite masses. Our group developed a method to correct the BO Hamiltonian by including effects of finite nuclear mass [41–44], which has been used to produce many results dependant on properties that arise because of the mass asymmetry. The most noteworthy for the development of the isotopic probe are the ones regarding the isotopic dipole moment [45–50], calculated via the ISOTOPE upgrade [49, 51] for the programs DALTON [52, 53] and GAMESS [54].

With this finite nuclear mass correction (FNMC), we can calculate the system's electric field by its influence on the probe, using the relation

$$U = -\vec{\mu} \cdot \vec{\mathbf{E}}, \tag{1.2}$$

being U the energy, $\vec{\mu}$ the probe's dipole moment, and $\vec{E}$ the molecular electrostatic field on the dipole.

The use of the electric field as an interactions quantifier is based on the Hellmann-Feynman theorem [55, 56], which states that the forces in molecules are all Coulombian in nature, i.e. arising from electrostatics and polarisation. This is the same principle that allows the use of the MEP as a quantifier, but the use of the probe gives us a more in-depth understanding of the interaction as a physical phenomenon.

The probe has the advantage of being as small as the smallest molecule, H_2, with only 1.4 a.u. of internuclear distance, so it can easily fit in regions of intermolecular interactions with distances larger than 3.55 a.u.[2]. We have chosen to use the probe to calculate the electric fields inside interactions involving π- and σ-holes, molecular regions

[2] This is the area of study of supramolecular chemistry, which is the field of chemistry that studies molecular assemblies and intermolecular bonds. It encompasses molecular devices and machines, molecular recognition, self-assembly and self-organisation, and has interfaces with the emergent fields of complex matter and nanochemistry [57].

that deserved much attention in the recent literature, as they represent a new kind of chemical bond [32]. π- and σ-holes are both regions of positive electrostatic potential that appear in some molecules, being able to make non-covalent bonds with negative sites of other molecules. They have been detected both in simple and complex molecular systems and the knowledge of their properties, mainly their strength, is very important for supramolecular chemistry.

For better understanding of the concepts and results presented, this thesis is organised as follows. Chapter 2 is an overview of the molecular approximations typically employed in quantum chemical calculations and the basis of the FNMC method, which allows us to calculate isotopic effects in molecules. Chapter 3 is an overview of the computational methods of calculation that we used in the process of refining the probe, and afterwards, in determining the strength of the interactions, namely HF, CI and DFT. Chapter 4 is a review of the work done in our lab about symmetry breaking in molecules, most importantly the work with isotopic dipole moments which inspired the creation of the isotopic probe. Chapter 5 shows the process of creation, calibration and programming of the probe, with preliminary results. Finally chapter 6 shows the calculations of electric fields inside molecules and systems of molecules of interest, and proposes the use of the electric field as a quantifier of molecular interactions. Chapter 7 gives a summary of what was discussed, and presents the plans for future work using the isotopic probe.

2 Molecular approximations

In this chapter, we will give an overview of a few molecular approximation theories. All this chapter is based on chapter 8 of reference [58], unless stated otherwise.

Since the periodic table of elements was developed, chemistry's knowledge began to be systematised around basic concepts, encompassed in the general concept of Molecular Structure. We consider the molecules to be made from atoms of chemical elements, that are classified based on their physical-chemical properties.

Our objective is to solve the time-independent non-relativistic Schrödinger equation, a task that we are not able to perform analytically for systems of the size we work with without approximations. One of such approximations consists in considering the electrons as moving and adapting to the movement of the nuclei almost instantly, adiabatically. This is called the *adiabatic model*, in which the electrons are light and fast, and the nuclei perceive only a mean field due to the electrons, aside from mutual repulsion. This means that the calculation of the electronic wave function takes into account the electron-nucleus interactions, but the coupling is not dynamic, there is no exchange of kinetic energy between electrons and nuclei. This creates a Potential Energy Surface (PES), which is where the nuclei move. The PES is the most fundamental instrument of physical-chemistry.

The adiabatic approximation allows us to separate electronic and nuclear movements, which happens when we introduce an electronic Hamiltonian operator, that depends parametrically on nuclear coordinates. The most utilized adiabatic approximation, the Born-Oppenheimer Approximation (BOA), considers static nuclei to solve the electronic problem.

We will use atomic units, defined by electron's mass, electron's charge, Bohr's radius and Planks constant all equal to the unity, i.e. $\mathrm{m} = \mathrm{e} = \mathrm{a}_0 = \hbar = 1$. This theory is non-relativistic.

2.1 Born-Huang theory

As noted above, our goal is to solve the non-relativistic time-independent Schrödinger equation

$$H\Psi(\mathbf{r}, \mathbf{R}) = E\Psi(\mathbf{r}, \mathbf{R}), \tag{2.1}$$

in which H is the Hamiltonian operator for a system of nuclei and electrons, $\mathbf{r}$ represents the coordinates for the electrons and $\mathbf{R}$ represents the coordinates of the nuclei. To solve equation (2.1) is to find a wave function that satisfies this relation when the operator H is

applied on it. For simplicity, we consider a diatomic molecule AB. The total Hamiltonian operator, in the laboratory reference frame (LAB) is

$$H = -\frac{\nabla_A^2}{2M_A} - \frac{\nabla_B^2}{2M_B} - \sum_i \frac{\nabla_i^2}{2} + V_{el} + \frac{Z_A Z_B}{R}, \tag{2.2}$$

A and B being the two nuclei, with masses M_A and M_B and charge Z_A and Z_B. The Laplace operator $\nabla^2_{A(B)}$ acts on the coordinates of nucleus A(or B) and the index i refers to the electrons. V_{el} represents electrostatic potentials for the electrons and the last term is the nuclei repulsion.

It is convenient to use a coordinate system with origin coinciding with the center of mass of the nucleus (hereafter known as MOL). This is done in order to eliminate translation for the system. In this system, the Hamiltonian is given by:

$$H = -\frac{\nabla_R^2}{2\mu_{AB}} - \sum_{i,j} \frac{1}{2M} \boldsymbol{\nabla}_i \cdot \boldsymbol{\nabla}_j - \sum_i \frac{\nabla_i^2}{2} + V, \tag{2.3}$$

in which $M = M_A + M_B$, $\mu_{AB} = \frac{M_A M_B}{M_A + M_B}$ is the nuclei reduced mass, ∇_R^2 is the Laplace operator relative to the nuclear coordinate and $V = V_{el} + \frac{Z_A Z_B}{R}$.

It is also usual to separate the Hamiltonian operator in two terms.

$$H = T_N + H_{el}, \tag{2.4}$$

T_N being the nuclear kinetic energy, and H_{el} being the electronic Hamiltonian that leads to the electronic basis functions. If we separate the operator in LAB, it leads directly to the BOA

$$H_{el} = H_{BO} \equiv -\sum_i \frac{\nabla_i^2}{2} + V, \tag{2.5}$$

but if we do the same in MOL, we get an operator that contains the nuclear mass [59]. First we need to define our wave function.

We can expand a generic wave function in a basis of electronic functions $\Phi_k(\mathbf{r}, \underline{\mathbf{R}})$ (the bar under R means that it is a parametric dependence),

$$\Psi(\mathbf{r}, \mathbf{R}) = \sum_k \chi_k(\mathbf{R}) \Phi_k(\mathbf{r}, \underline{\mathbf{R}}) = \sum_k \chi_k \Phi_k. \tag{2.6}$$

The coefficients χ_k are the nuclear functions obtained as we solve equation 2.1.

Now we must substitute equations (2.6) and (2.3) in equation (2.1),

$$\left[-\frac{\nabla_R^2}{2\mu_{AB}} - \sum_{i,j} \frac{1}{2M} \boldsymbol{\nabla}_i \cdot \boldsymbol{\nabla}_j - \sum_i \frac{\nabla_i^2}{2} + V \right] \sum_k \chi_k \Phi_k = E \sum_k \chi_k \Phi_k. \tag{2.7}$$

We then apply the following Laplace operator property: $\nabla_R^2\chi\Phi = \Phi\nabla_R^2\chi+\chi\nabla_R^2\Phi+2\boldsymbol{\nabla}_R\phi\cdot\boldsymbol{\nabla}_R\chi$, and we get

$$\sum_l \left\{-\frac{1}{2\mu_{AB}}\left[\Phi_l\nabla_R^2\chi_l + (\nabla_R^2\Phi_l)\chi_l + 2\boldsymbol{\nabla}_R\Phi_l\cdot\boldsymbol{\nabla}_R\chi_l\right]\right\} - \sum\left\{\frac{1}{2M}\left(\sum_{i,j}\boldsymbol{\nabla}_i\cdot\boldsymbol{\nabla}_j\right)\chi_l + \frac{1}{2}\chi_l\sum_i\nabla_i^2\Phi_l - V\Phi_l\chi_l\right\} = E\sum_l\Phi_l\chi_l. \quad (2.8)$$

Now we left multiply by Φ_k^* and integrate over the electronic coordinates, which is what we symbolise by $\langle\,\rangle$, and we have

$$\sum_l\left[-\frac{1}{2\mu_{AB}}(\langle\Phi_k|\Phi_l\rangle\,\nabla_R^2\chi_l + \langle\Phi_k|\nabla_R^2|\Phi_l\rangle\,\chi_l + 2\,\langle\Phi_k|\boldsymbol{\nabla}_R|\Phi_l\rangle\cdot\boldsymbol{\nabla}_R\chi_l)\right] + \sum_l\left[-\frac{1}{2M}\sum_{i,j}\langle\Phi_k|\boldsymbol{\nabla}_i\cdot\boldsymbol{\nabla}_j|\Phi_l\rangle\,\chi_l - \frac{1}{2}\sum_i\langle\Phi_k|\nabla_i^2|\Phi_l\rangle + \langle\Phi_k|V|\Phi_l\rangle\,\chi_l\right] = E\sum_l\langle\Phi_k|\Phi_l\rangle\,\chi_l. \quad (2.9)$$

Considering an orthonormal basis, $\langle\Phi_k|\Phi_l\rangle = \delta_{kl}$, and adopting the notation $\langle\Phi_k|A|\Phi_l\rangle = A_{kl}$, we then arrive to

$$\left\{-\frac{1}{2\mu_{AB}}[\nabla_R^2 + (\nabla_R^2)_{kk} + 2(\boldsymbol{\nabla}_R)_{kk}\cdot\boldsymbol{\nabla}_R] - \frac{1}{2M}(\sum_{i,j}\boldsymbol{\nabla}_i\cdot\boldsymbol{\nabla}_j)_{kk} - \frac{1}{2}(\sum_i\nabla_i^2)_{kk} + V_{kk} - E\right\}\chi_k = \sum_{l\neq k}\left\{\frac{1}{2\mu_{AB}}[(\nabla_R^2)_{kl} + 2(\boldsymbol{\nabla}_R)_{kl}\cdot\boldsymbol{\nabla}_R] + \frac{1}{2M}(\sum_{i,j}\boldsymbol{\nabla}_i\cdot\boldsymbol{\nabla}_j)_{kl} + \frac{1}{2}(\sum_i\nabla_i^2)kl - V_{kl}\right\}\chi_l, \quad (2.10)$$

in which we have separated diagonal terms on the left, and non-diagonal terms on the right. Finally we can write

$$\left\{-\frac{\nabla_R^2}{2\mu_{AB}} + H_{kk} - \frac{(\boldsymbol{\nabla}\cdot_R)_{kk}\cdot\boldsymbol{\nabla}_R}{\mu_{AB}} - E\right\}\chi_k = \sum_{l\neq k}\left\{-H_{kl} + \frac{(\boldsymbol{\nabla}_R)_{kl}\cdot\boldsymbol{\nabla}_R}{\mu_{AB}}\right\}\chi_l. \quad (2.11)$$

This is a set of coupled equations, whose solution gives the nuclear functions χ_k, and consequently, via equation (2.6), total wave functions and molecular energies. Electronic functions are already known in this stage (eigenfunctions of H_{el}) and they depend on the particular choice of H_{el}. Although the solution for equation (2.11) is usually non-viable, this set of equations is the starting point for more viable approximations, like the adiabatic approximation.

2.2 Adiabatic approximation

If we assume the complete decoupling of electronic states, only one term is left in equation (2.6) for each molecular state,

$$\Psi \equiv \Psi_{ad} = \chi_k \Phi_k, \tag{2.12}$$

and we have what is called the adiabatic approximation. With this approximation, the coupling terms vanish and equations (2.11) reduce to

$$\left\{ -\frac{\nabla_R^2}{2\mu_{AB}} + H_{kk} - \frac{(\boldsymbol{\nabla}_R)_{kk} \cdot \boldsymbol{\nabla}_R}{\mu_{AB}} - E \right\} \chi_k = 0. \tag{2.13}$$

As for the validity of this approximation, it is possible to show that the non diagonal coupling terms involve the energy difference of the states in question [58]. That means that the more isolated a state is, the better the approximation for said state, which is usually the case for ground states.

The above equation represents, for a given k, Schrödinger's equation for a particle of mass μ_{AB} moving in a potential $U_k(R)$,

$$U_k(R) = H_{kk} - \frac{(\boldsymbol{\nabla}_R)_{kk} \cdot \boldsymbol{\nabla}_R}{\mu_{AB}}. \tag{2.14}$$

This means that $U_k(R)$ represents the PES for nuclear movement. The second term is called *diagonal coupling of nuclear moments*. This term is usually small, due to the presence of μ_{AB} in the denominator. If the electronic functions are normalised,

$$\langle \Phi_k | \Phi_k \rangle = 1 \Rightarrow \boldsymbol{\nabla}_R \langle \Phi_k | \Phi_k \rangle = 0, \tag{2.15}$$

and, if they are real

$$(\boldsymbol{\nabla}_R)_{kk} = \langle \Phi_k | \boldsymbol{\nabla}_R | \Phi_k \rangle = 0. \tag{2.16}$$

This result nullifies the second term in $U_k(R)$. It is possible to redefine Φ_k, if they are complex, by multiplying by a phase A(R), so that the above relation remains valid. This is usually assumed in adiabatic calculations and it is true for isolated PES. Therefore, we consider the diagonal coupling term null. Our PES is then given by

$$U_k(R) = H_{kk}. \tag{2.17}$$

The choice of H_{el}, which defines the basis $\{\Phi_k\}$, is called a *representation*. For each chosen representation we get a particular set $U_k(R)$ with its respective set of electronic states.

2.3 The Born-Oppenheimer approximation

The BO representation is defined by making the nuclear masses tend to infinity in H, i.e.

$$H_{el} = H_{BO} = -\sum_i \frac{\nabla_i^2}{2} + V, \tag{2.18}$$

$$H_{BO}\Phi_k = (\epsilon_{BO})_k \Phi_k. \tag{2.19}$$

The coupled equations (2.11) become

$$\left\{ -\frac{\nabla_R^2}{2\mu_{AB}} + (\epsilon_{BO})_k + \left(-\frac{\nabla_R^2}{2\mu_{AB}} - \sum_{i,j} \frac{\boldsymbol{\nabla}_i \cdot \boldsymbol{\nabla}_j}{2M} \right)_{kk} - E \right\} \chi_k = \sum_{l \neq k} \left\{ \left(\frac{\nabla_R^2}{2\mu_{AB}} + \sum_{i,j} \frac{\boldsymbol{\nabla}_i \cdot \boldsymbol{\nabla}_j}{2M} \right)_{kl} + \frac{(\boldsymbol{\nabla}_R)_{kl} \cdot \boldsymbol{\nabla}_R}{\mu_{AB}} \right\} \chi_l. \tag{2.20}$$

and, in the BO adiabatic approximation, we have the following nuclear equation:

$$\left\{ -\frac{\nabla_R^2}{2\mu_{AB}} + (\epsilon_{BO})_k + \left(-\frac{\nabla_R^2}{2\mu_{AB}} - \sum_{i,j} \frac{\boldsymbol{\nabla}_i \cdot \boldsymbol{\nabla}_j}{2M} \right)_{kk} - E \right\} \chi_k = 0. \tag{2.21}$$

The BOA is an infinite nuclear mass approximation. If we take infinite nuclear masses in the H_{BO} operator, i.e. the electronic part of (2.21) (recall that the first term is T_N from (2.4)), that leads to

$$\left\{ -\frac{\nabla_R^2}{2\mu_{AB}} + (\epsilon_{BO})_k - E \right\} \chi_k = 0. \tag{2.22}$$

The PES are generated by the electronic energies $U_k(\mathbf{R}) = (\epsilon_{BO})_k(\mathbf{R})$ added to the nuclear repulsion terms.

2.4 The adiabatic correction

As we have seen, in the BOA, neither the electronic functions, nor the PES have information about nuclear masses. We can correct the PES with the Diagonal Born-Oppenheimer Correction (DBOC), also called adiabatic correction,

$$DBOC(\mathbf{R}) = \left(-\frac{\nabla_R^2}{2\mu_{AB}} - \sum_i \frac{\nabla_R^2}{2M} - \sum_{i \neq j} \frac{\boldsymbol{\nabla}_i \cdot \boldsymbol{\nabla}_j}{2M} \right)_{kk}. \tag{2.23}$$

The PES is corrected in this procedure, but not the wave function, which remains with no isotopic signature. DBOC is specially important in systems with hydrogen atoms.

2.4.1 The model Hamiltonian operator

An alternative to DBOC that makes the electronic wave functions dependent on the nuclear masses is the so called FNMC [43,51]. This is the basis of most of the research in our group. Also based on chapter 8 of reference [58].

Starting from the Hamiltonian operator for a molecule with m nuclei and n electrons in LAB,

$$H = -\sum_{i}^{n} \frac{1}{2}\nabla_i^2 - \sum_{A}^{m} \frac{1}{2M_A}\nabla_A^2 + V = -\sum_{A}^{m} \frac{\nabla_A^2}{2M_A} + H_{BO}, \tag{2.24}$$

conservation of linear momentum on a generic atom, A, implies $\boldsymbol{\nabla}_A = -\sum_i^{n_A} \boldsymbol{\nabla}_i$ and $\nabla_A^2 \approx \sum_i^{n_A} \nabla_i^2$, in which we have neglected terms $i \neq j$, because they are much smaller than the $i = j$ ones. In MOL, this equation becomes

$$H = -\sum_{j=1}^{n_A} \frac{1}{2M_A}\nabla_j^2 - \sum_{k=n_A+1}^{n_A+n_B} \frac{1}{2M_B}\nabla_k^2 + ... - \sum_{i=1}^{N} \frac{1}{2}\nabla_i^2 + V. \tag{2.25}$$

This is a purely electronic Hamiltonian operator, with n_A representing the electrons of nucleus A and n_B representing the electrons of nucleus B; but since each electron was assigned to a specific nucleus, this violates the principle of the indistinguishability for the electrons.

To solve this problem, we postulate that the matrix elements are null when it deals with different atoms. We use a projector, P_A, in order to do that, and we define the model Hamiltonian operator as

$$H = \sum_{A}^{m} \left(-\sum_{i,j}^{n} P_A \frac{\boldsymbol{\nabla}_i \cdot \boldsymbol{\nabla}_j}{2m_A} P_A \right) - \sum_{i}^{N} \frac{1}{2}\nabla_i^2 + V, \tag{2.26}$$

in which P_A projects the full electronic wave function over the space of atomic functions of nucleus A.

Using this approximation, both the PES and the states have being adiabatically corrected, and we can use it to study effects of finite nuclear mass during the electronic calculation.

This approximation is a central component of this work, since we need to be able to calculate isotopic dipole moments and it cannot be done using BOA alone. The origin of this effect is the difference between the Bohr's radii of isotopes. An example is the molecule of HD (D = deuterium). This molecule presents a dipole moment because D atoms have a smaller Bohr radius than H atoms. It is a very small dipole moment, when compared with polar molecules, as we can see in table 1. Vibrational effects increase the dipole moment [48], but they are not relevant in this work, because we use a static dipole. Previous calculations were performed for CH_3CD_3 e SiH_3SiD_3 and compared with experimental spectroscopy results, with accuracy within 10^{-4} debye [49], for which the inclusion of the purely electronic effects has shown to be fundamental..

Table 1 – Dipole moments for HD and some polar diatomic molecules.

Molecule	Dipole moment (debye)
H_2O	1.855
LiH	5.880
HF	1.820
HD	$8.1x10^{-4}$

Source – Reference [60]

3 Computational Methods

In this chapter, we will give a brief overview of the computational methods used in this thesis for electronic calculations, i.e. Hartree-Fock (HF), Configuration Interaction (CI), and Density Functional Theory (DFT). This chapter is based on reference [58], unless stated otherwise.

3.1 Hartree-Fock

As stated in the last chapter, in general, it is impossible to determine the real solution to the Schrödinger equation, and we must use approximations. The HF method is the most popular computational method employed to determine approximate solutions to the electronic problem. It has the advantage of being used as a starting point for other methods, like the CI method that we will discuss in a following section.

Since the electrons are indistinguishable fermions, the describing wave function is required to be antisymmetric with respect to the exchange of the global coordinates of two electrons. We can use a determinant to generate a valid antisymmetric wave function, because determinants are antisymmetric by default. This determinant of spin orbitals is called a Slater Determinant:

$$\Phi_0 = \frac{1}{\sqrt{N!}} \begin{vmatrix} \chi_1(\mathbf{x}_1) & \chi_2(\mathbf{x}_1) & \cdots & \chi_N(\mathbf{x}_1) \\ \chi_1(\mathbf{x}_2) & \chi_2(\mathbf{x}_2) & \cdots & \chi_N(\mathbf{x}_2) \\ \vdots & \vdots & & \vdots \\ \chi_1(\mathbf{x}_N) & \chi_2(\mathbf{x}_N) & \cdots & \chi_N(\mathbf{x}_N) \end{vmatrix}, \tag{3.1}$$

in which the χs are one electrons spatial and spin functions, and $1/\sqrt{N!}$ is a normalisation constant.

Exchange of two electrons is the same as exchanging two lines of the determinant, which implies the inversion of the determinant's sign. In other words, the HF wave function defined in terms of a Slater determinant is antisymmetric with respect to the exchange of the global coordinates of two electrons. It is also zero if two molecular spin-orbitals are the same, represented by two columns being equal to each other in the determinant, a characteristic required by Pauli's exclusion principle.

For each spatial orbital, there are two possible spin orbitals:

$$\chi(\mathbf{x}) = \begin{cases} \phi(\mathbf{r})\alpha(1) \\ \phi(\mathbf{r})\beta(1) \end{cases} , \tag{3.2}$$

α and β representing up-spin and down-spin, respectively, and ϕ being one electron spatial functions. The method is called Unrestricted Hartree-Fock(UHF), if we make no restrictions to the orbitals. If we impose the restriction that every orbital has to have two electrons, one with up-spin and one with down-spin, the method is called Restricted Hartree-Fock (RHF). There is also a Resctricted Open-Shell Hartree-Fock (ROHF) which is an attempt at using a restricted wave function to describe a system with unpaired electrons.

We have to calculate the energy of the system, i.e. the expected value of the Hamiltonian

$$E = \langle \Phi | H | \Phi \rangle , \tag{3.3}$$

and we know, from the variational principle, that this approximate energy is an upper bound on the true energy of the system. So we vary the parameters of $|\Phi\rangle$ in order to minimise the energy.

But first we'll write the Hamiltonian in a different way, separating the one electron and the two electron parts

$$H = O_1 + O_2, \tag{3.4}$$

being

$$O_1 = \sum_{i=1}^{N} h(i), \tag{3.5}$$

with

$$h(i) = -\frac{1}{2}\nabla_i^2 - \sum_{A=1}^{M} \frac{1}{r_{iA}}, \tag{3.6}$$

and

$$O_2 = \sum_{i=1}^{N} \sum_{j>i}^{N} \frac{1}{r_{ij}}. \tag{3.7}$$

With some algebraic tricks we can write the HF energy in terms of one and two electron integrals

$$E = \sum_{a}^{N} \langle \chi_a | h | \chi_a \rangle + \frac{1}{2} \sum_{a,b}^{N} [\langle \chi_a \chi_b | \chi_a \chi_b \rangle - \langle \chi_a \chi_b | \chi_b \chi_a \rangle], \tag{3.8}$$

in which $\langle \chi_a \chi_b | \chi_a \chi_b \rangle$ is short for

$$\langle \chi_a \chi_b | \chi_a \chi_b \rangle = \langle \chi_a \chi_b | \frac{1}{r_{ab}} | \chi_a \chi_b \rangle . \tag{3.9}$$

So, in order to calculate the energy (3.3), we must minimise the energy expression (3.8) with respect to changes in the orbitals $\chi_i \to \chi_i + \delta\chi_i$. We can use Lagrange's method of undetermined multipliers which consists in minimising the functional

$$L[\chi] = E[\chi] - \sum_{a,b} \epsilon_{ba}(\langle\chi_a|\chi_b\rangle - \delta_{ab}). \tag{3.10}$$

We impose the condition for L to be real, and with that the multipliers must constitute elements of an hermitian matrix. After some more algebra, we get

$$\delta L = \sum_a \langle\delta\chi_a|\, h\,|\chi_a\rangle + \sum_{a,b}\{\langle\delta\chi_a\chi_b|\chi_a\chi_b\rangle - \langle\delta\chi_a\chi_b|\chi_b\chi_a\rangle\} - \sum_{a,b} \epsilon_{ba}\,\langle\delta\chi_a|\chi_b\rangle + c.c., \tag{3.11}$$

and then we can define the Coulomb and exchange operators, respectively $\mathcal{J}_b$ and $\mathcal{K}_b$:

$$\mathcal{J}_b(1)\chi_a(1) = \langle\chi_b(2)|\frac{1}{r_{12}}|\chi_b(2)\rangle\,\chi_a(1), \tag{3.12}$$

$$\mathcal{K}_b(1)\chi_a(1) = \langle\chi_b(2)|\,\frac{1}{r_{12}}\,|\chi_a(2)\rangle\,\chi_b(1), \tag{3.13}$$

so we can write

$$\delta L = \sum_a |\delta\chi_a(1)\rangle \left\{ \left[h(1) + \sum_b [\mathcal{J}_b(1) - \mathcal{K}_b(1)]\right] |\chi_a(1)\rangle - \sum_b \epsilon_{ba}\,|\chi_b(1)\rangle \right\} + c.c.. \tag{3.14}$$

We need $\delta L = 0$ for L to have a minimum, which is equivalent to making

$$\left\{h(1) + \sum_b [\mathcal{J}_b(1) - \mathcal{K}_b(1)]\right\}\chi_a(1) = \sum_b \epsilon_{ba}\chi_b(1). \tag{3.15}$$

The term between braces is called the Fock operator $\mathcal{F}$:

$$\mathcal{F}(1) = h(1) + \sum_b [\mathcal{J}_b(1) - \mathcal{K}_b(1)]. \tag{3.16}$$

Now, the HF equations are only

$$\mathcal{F}(1)\chi_a(1) = \sum_b \epsilon_{ba}\chi_b(1), \tag{3.17}$$

and for trial functions we can use a linear combination of atomic orbitals (LCAO):

$$\phi_p(r) = \sum_\nu = 1^k C_{\nu p} g_\nu(r), \tag{3.18}$$

k being the number of functions and $C_{\nu p}$ are coefficients to be determined. And by plugging this into the HF equations, we can obtain the Rootham equations:

$$\mathbf{F}'\mathbf{C}' = \mathbf{C}'\epsilon, \tag{3.19}$$

which is a canonical eigenvalue equation and can be easily solved, being ϵ the diagonal matrix of the orbital energies ϵ_i and S the overlap matrix.

3.2 Configuration Interactions

RHF suffers from a problem when calculating dissociation energies for molecules whose fragments have open shells. An example would be the hydrogen molecule with spin-orbitals $1\sigma_g\alpha$ and $1\sigma_g\beta$, i.e. given by the Slater determinant $\left|1\sigma_g\alpha \quad 1\sigma_g\beta\right|$. The molecular orbital can be expressed as a LCAO, a combination of two atomic functions:

$$1\sigma_g = C(1s_A + 1s_B). \tag{3.20}$$

We can expand the determinant as

$$\begin{aligned} D_0 = C^2\{1s_A(r_1)1s_A(r_2) + 1s_B(r_1)1sB(r_2) + 1s_A(r_1)1s_B(r_2) \\ + 1s_B(r_1)1s_A(r_2)\} \times \{\alpha_1\beta_2 - \beta_1\alpha_2\}/\sqrt{2}, \end{aligned} \tag{3.21}$$

with the first two terms corresponding to $H_A^- + H_B^+$ and $H_A^+ + H_B^-$, and the last two terms corresponding to the dissociation responsible for the RHF problem. We could use UHF to deal with this, but other problems arise.

What we'll do is use more Slater determinants to write the wave function, for example, we could use two:

$$\Psi(x_1, x_2) = c_0 D_0(x_1, x_2) + c_1 D_1(x_1, x_2), \tag{3.22}$$

in which

$$D_1(x_1, x_2) = \left|1\sigma_u\alpha \quad 1\sigma_u\beta\right|, \tag{3.23}$$

and

$$1\sigma_u = C(1s_A - 1s_B). \tag{3.24}$$

By using this D_1 determinant, we lower the total energy of the system compared to using only D_0, as table 2 shows. The difference in the energy is called *electronic correlation energy*, and this is the basis of the CI method, the use of more Slater determinants to write the wave function, in order to correct the HF energy. The CI wave function is an expansion of Slater determinants, that can be generated as all the possible excitations of electrons of one of more occupied orbitals to the virtual orbitals created by the basis used.

Table 2 – HF and CI energies for the wave function from equation (3.22).

$R/$	E_{HF}	E_{CI}
0.80	-0.947308	-0.97599
0.90	-1.019497	-1.031043
1.00	-1.065999	-1.078970
1.10	-1.094564	-1.109137
1.20	-1.110334	-1.126699

Source – Adapted from reference [58]

This, of course, makes this method not practical for systems with more than 20 electrons, due to the expansion having an excessive number of terms. To easily indicate the number of excitations used in the calculation, the terminology created by the users is very clear: *CISD* for single and double excitations, or *full-CI* for all the possible excitations, for example.

A critique to the method is CI not being size-consistent, that is, the sum of the energies from the system's fragments is not equal to the energy of the system

$$E_{AB-XY} \neq E(AB) + E(XY). \tag{3.25}$$

Some chemists argue that this is not a harmful problem, because they rarely calculate energies using CISD starting from a HF determinant, which makes the difference negligible.

3.3 Density Functional Theory

DFT was a paradigm change in computational chemistry since the publishing of the Hohenberg and Kohn theorems in 1964 [61], in which they demonstrate that the electron density could be used in place of spatial coordinates in order to perform quantum chemistry calculations, which could facilitate the computation for large systems.

Starting from the electronic BO molecular Hamiltonian, (2.18), we separate the potential V in two terms, one representing the external potential, U, which we'll write as

$$U = \sum_{i}^{N} \sum_{A}^{M} -\frac{Z_A}{R_A - R_i} = \sum_{i}^{N} v(\mathbf{r}_i), \tag{3.26}$$

and a repulsion term, V_e, which we'll write as

$$V_e = \sum_{i<j}^{N} \sum_{j}^{N} \frac{1}{|\mathbf{r}_i - \mathbf{r}_j|}. \tag{3.27}$$

The electron density can be written as

$$\rho(r) = \int \cdots \int \Psi(\mathbf{r}_1, \mathbf{r}_2, \cdots, \mathbf{r}_N) * \Psi(\mathbf{r}_1, \mathbf{r}_2, \cdots, \mathbf{r}_N) \mathrm{d}\mathbf{r}_1 \mathrm{d}\mathbf{r}_2 \cdots \mathrm{d}\mathbf{r}_N, \tag{3.28}$$

with $\Psi(r_1, r_2, \cdots, r_N)$ being the solution to the ground state Hamiltonian.

The external potential U can be separated in a trivial functional of the electron density, so that the energy of the system can be written as:

$$E_0 = \langle \Psi | T + V_e | \Psi \rangle + \int \rho(\mathbf{r}) v(\mathbf{r}) \mathrm{d}r, \tag{3.29}$$

with T being the kinetic energy. We can see now that the number of electrons, N, and the external potential, define completely the Hamiltonian of the system.

Hohenberg-Kohn's first theorem states that the external potential is a unique functional of $\rho(r)$ plus an additive constant. In other words, we can use the density in order to determine the number of electrons and the potential, both of which can be used to determine the Hamiltonian and then calculate the energy of the system.

Hohenberg-Kohn's second theorem establishes that any approximate functional will generate an approximate energy that's an upper bound to the exact energy of the system, since each $\tilde{\rho}(r)$ generates its own $\tilde{v}(r)$ that will be used to calculate the energy.

The two theorems show how we can use the density in place of the N-electron wave function to determine the state of the system, so instead of 3N variables for each electron, we have only the three coordinates of the density. The first problem with that method is to guarantee that $\tilde{\rho}(r)$ is v-representable and N-representable. Being v-representable is to guarantee that $\tilde{\rho}(r)$ can determine the real external potential, and being N-representable is to guarantee that $\tilde{\rho}(r)$ can be generated by an anti symmetric wave function. The density is always N-representable if the following conditions are satisfied:

$$\rho(\mathbf{r}) \geq 0, \tag{3.30}$$

$$\int \rho(\mathbf{r}) \mathrm{d}\mathbf{r} = N, \tag{3.31}$$

$$\int |\boldsymbol{\nabla} \rho(\mathbf{r})^{1/2}|^2 \mathrm{d}\mathbf{r} < \infty. \tag{3.32}$$

The v-representability can be sidestepped with Levy Constrained Search:

$$F[\rho] = \langle \Psi_o | T + V | \Psi_o \rangle = \min_{\Psi \to \rho} \langle \Psi_o | T + V | \Psi_o \rangle, \tag{3.33}$$

that is, performing the Constrained Search is testing all the tentative densities and, for each of them, find the wave functions that minimise F[ρ][1].

We have to follow Kohn and Sham method to solve DFT problems without any loss of accuracy [62]. This consists in mapping the system of interacting electrons onto a

[1] In this equation, the wave function does not tend to ρ, it means that the functional takes the minimum value of the expectation value with respect to all states Ψ which give the density ρ.

system on non-interacting "electrons"

$$\delta\left\{E_v[\rho] - \mu\left[\int \rho(\mathbf{r})\mathrm{d}\mathbf{r} - N\right]\right\} = 0. \tag{3.34}$$

Kohn and Sham separated the above equation into three parts, making explicit the Coulomb electron-electron repulsion and defining a new function G[ρ]:

$$E_v[\rho] = G[\rho] + \frac{1}{2}\int\int \frac{\rho(\mathbf{r}_1)\rho(\mathbf{r}_2)}{|\mathbf{r}_1 - \mathbf{r}_2|}\mathrm{d}\mathbf{r}_1\mathrm{d}\mathbf{r}_2 + \int \rho(\mathbf{r})v(\mathbf{r})\mathrm{d}\mathbf{r}, \tag{3.35}$$

in which

$$G[\rho] = T_s[\rho] + E_{xc}[\rho], \tag{3.36}$$

and $T_s[\rho]$ is the kinetic energy functional for the non-interacting "electron" system.

It is possible to use this system with a Hamiltonian that has an effective potential, $v_{ef}(r)$

$$H^{KS} = -\frac{1}{2}\nabla^2 + v_{ef}(\mathbf{r}). \tag{3.37}$$

The wave function is obtained the same way we obtained it in HF, equation (3.1). Therefore, Kohn-Sham orbitals are obtained from the one electron Schrödinger equation:

$$\left(-\frac{1}{2}\nabla^2 + v_{el}\right)\psi_i^{KS} = \epsilon_i\psi_i^{KS}. \tag{3.38}$$

We then choose the effective potential in a way to make the density equal to the fundamental electron density:

$$\rho_s = \sum_i^N 2|\psi_i^{KS}|^2 = \rho_0(\mathbf{r}). \tag{3.39}$$

We calculate the kinetic energy using a self-consistent method,

$$T_s[\rho] = \sum_i^N \left\langle \psi_i^{KS}\middle| -\frac{1}{2}\nabla_i^2 \middle|\psi_i^{KS}\right\rangle, \tag{3.40}$$

and we minimise it to obtain the effective potential, with the restriction that the one electron functions are orthonormal:

$$v_{ef}(\mathbf{r}) = v(\mathbf{r}) + \int \frac{\rho(\mathbf{r}_1)}{|\mathbf{r} - \mathbf{r}_1|}\mathrm{d}\mathbf{r}_1 + v_{xc}(\mathbf{r}), \tag{3.41}$$

with

$$v_{xc}(\mathbf{r}) = \frac{\delta E_{xc}[\rho]}{\delta\rho(\mathbf{r})}. \tag{3.42}$$

The self-consistent method to solve the Kohn-Sham equations is

a) Choosing the initial set of Kohn-Sham orbitals ψ_i^0

b) Calculation of the electron density, equation (3.39)

c) Calculation of the Kohn-Sham effective potential, equation (3.41)

d) Solving Schödinger's equation with Hamiltonian (3.37) and forming a new set of one electron functions ψ_i^d

e) Convergence check

   – if positive, terminate

   – if negative, replace ψ_i^0 with ψ_i^d and go to b

f) Termination: calculation of the final energy and other properties

4 Breaking nuclear mass symmetry

The Stanford Encyclopedia of Philosophy defines symmetry in modern science as "invariance under specified groups of rotations and reflections" [63], and it is useful to think about it in terms of group theory, especially in the case of molecules. Symmetry can be broken, though, but that does not mean that the system is no longer symmetric, it just has a state with lower symmetry than the original. This is important in the field of quantum chemistry, because many properties can be described as arising from a symmetry breaking. In this chapter, we will explore a specific type of symmetry breaking in molecular physics, the symmetry breaking of nuclear mass, done at LATME (Laboratório de Atomos e Moléculas Especiais; *special atoms and molecules laboratory*), and its most important consequence for our work: the isotopic dipole moment.

Our groups work with symmetry breaking on molecules started in 1999, when professor Mohallem showed that by using a Modified Electronic Mass Correction (MEMC) in the electronic Hamiltonian, it became possible to correct the BO energy for the adiabatic effect, even accounting for isotopic effects [41]. Later it was shown that this approach could generate results comparable to the diagonal Born-Oppenheimer correction (DBOC) [42] and was generalised to bigger molecules [44].

The method was renamed FNMC, and was able to show symmetry breaking effects in isotopologues (molecules containing isotopic substitution), when it was considered not possible for any methods beyond the BOA to observe point group symmetry [64]. The symmetry breaking arises from the different nuclear mass. For example, in water, when we replace a hydrogen atom (H) for a deuteron (D), the molecule loses part of its symmetry, and the resulting HDO molecule only has the identity symmetry operation [45, 64]. This is responsible for a small dipole moment, that can be verified by Mulliken population analysis (D has higher electron population than H). The dipole moment of HDO was later calculated in the equilibrium geometry [46] and with zero-point vibrational correction [50]. Isotopologue water clusters' dipole moments were studied in 2010 by Mohallem [65]

In 2008, Diniz and Mohallem studied the effects of symmetry breaking in hydrogen dimers and isotopologues [47], and were able to identify that the most stable configurations for the systems is a T configuration (meaning one molecule perpendicular to the other), as can be seen in Figure 2. We can see that the dipoles, when they exist, do not align, meaning that this effect is smaller than the rest of the interactions, which justified the future use of isotopic masses.

The dipole moment (DM) is a very important observable, which is used experimentally as a means to measure the polarity of a chemical interaction, i.e., the separation of

Figure 2 – T configuration for hydrogen dimer and isotopologues.

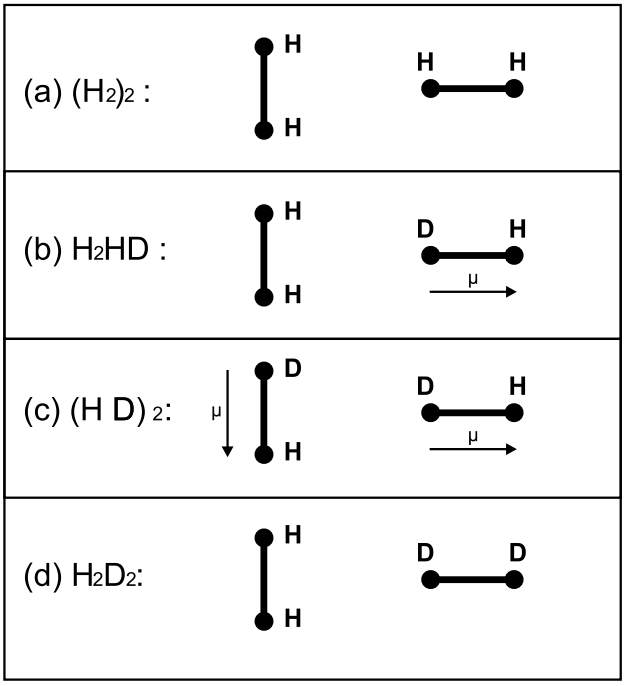

The T configuration for the dimers, with the dipole moments' direction shown.

Source – Adapted from [47]

the positive and negative centers of charge in the molecule. It is measured via the electric field - dipole moment coupling

$$U = -\mu \cdot \vec{\mathbf{E}}. \tag{4.1}$$

The electronegativity is the ability for the nucleus to attract electrons, and the atomic property that normally defines the dipole moment in molecules. It is unique for each different nucleus, which means that when two elements interact, the difference in electronegativity causes the electron cloud to shift slightly from the less electronegative element (leaving it with charge $-\delta$) to the more electronegative element (leaving it with charge $+\delta$). Each interaction has a dipole moment which may be represented by a vector pointing in the direction $-\delta \rightarrow +\delta$, and the molecular dipole moment is the sum of each of those. Many molecules have permanent dipole moment, and are called polar molecules, e.g. H_2O, HCl, O_3, NH_3. Other molecules can have the dipole moment induced by an external electric field, but show no permanent dipole, as is the case of diatomic molecules with the same two atoms, since the two atoms have the same electronegativity, and thus, have net charge displacement equal to zero. The criteria we use to differentiate atoms is the number of protons in the nucleus: atoms with the same number of protons are of the same element, and that is what was later denominated as the atomic number. However, the nucleus contains not only protons, but also neutrons that, although have no charge, also have an impact on electronic properties (albeit a small one) and can be in different

number between two atoms even if they are of the same element. These atoms that are classified as being of the same element, by having the same number of protons, but have a different number of neutrons, are called isotopes [66].

As we have seen in chapter 2, if you calculate electronic problems using only the BOA, you cannot differentiate between isotopes, because the BOA considers that the nucleus have infinite masses, thus there is no way to add or remove neutrons. So we chose to use the model Hamiltonian operator (2.26), which can calculate isotopic electronic properties, due to its consideration of the nuclear masses in the calculations.

Arapiraca [48] made a very thorough review of isotopic dipole moments. He calculated the dipole moment of isotopologues of hydrogen, ethane, ethilene, propane, propyne, benzene, water, and used his calculations to create rotational spectra for ones with astrophysical interest [49, 50, 67]. His work and expertise helped us immensely in the first stages of the development of the probe, although we did not use ro-vibrational corrections when calculating properties with the probe.

5 The isotopic probe

The purpose of this work is to develop a novel way of analysing molecular environments and quantifying intermolecular interactions. We do this by programming and using a fictitious probe in quantum chemistry calculations, together with a system of interest. The probe is a virtual molecule, programmed as an HD-like molecule, but with variable nuclear masses. Its HD-"likeness" comes from the fact that the probe has two atoms, each with one proton, same equilibrium distance as HD, and two electrons; but the "protons" don't have the usual proton mass, they each have a different mass. We will go into more detail later in this chapter.

The virtual probe was built this way because we needed a small dipole moment to align itself with the electric fields generated by near systems, since all intermolecular interactions can, in principle, be studied by a Coulombic point of view [33–35], i.e. electrostatics plus polarisation. This is done already in many methods of analysis which rely on the MEP as a pointer for different molecular regions.

5.1 The Molecular Electrostatic Potential

The MEP is a physical observable, and it is used to calculate electrical properties of molecular systems since computer efficiency increased enough to perform accurate electronic structure calculations [6], it is given by

$$V(\mathbf{r}) = \sum_A \frac{Z_A}{|\vec{\mathbf{R}}_A - \vec{\mathbf{r}}|} - \int \frac{\rho(\vec{\mathbf{r}}')\mathrm{d}^3 r'}{|\vec{\mathbf{r}} - \vec{\mathbf{r}}'|}, \tag{5.1}$$

being Z_A and R_A the charge and position of nucleus A, respectively, and $\rho(\mathbf{r}')$ the electronic density. Figure 3, from ref. [3], depicts this procedure. It is simple to calculate using modern computers, only limited by the quality of $\rho(\mathbf{r}')$'s description, which is heavily dependent on the basis used [7]. Besides, it does not take into account approaching molecules and their effects, and it also cannot give information about the nature of the second molecule [8,36]. Nonetheless, the MEP is the basic observable to calculate properties of electrostatic nature in quantum chemistry.

Since $\rho(\mathbf{r})$ has to be determined in order to calculate the MEP, one must choose a method to do so. One of the first methods proposed, if not the first, was the method of point charges. This method consists in representing atoms by point charges [9–13]. Questions arose about the validity of such representations, because there is not a unique way to determine what charge to assign to each atom, in order to best approach $\rho(\mathbf{r})$. It can be chosen, for example, based on electrostatic models, population analysis, and

Figure 3 – Electrostatic potential

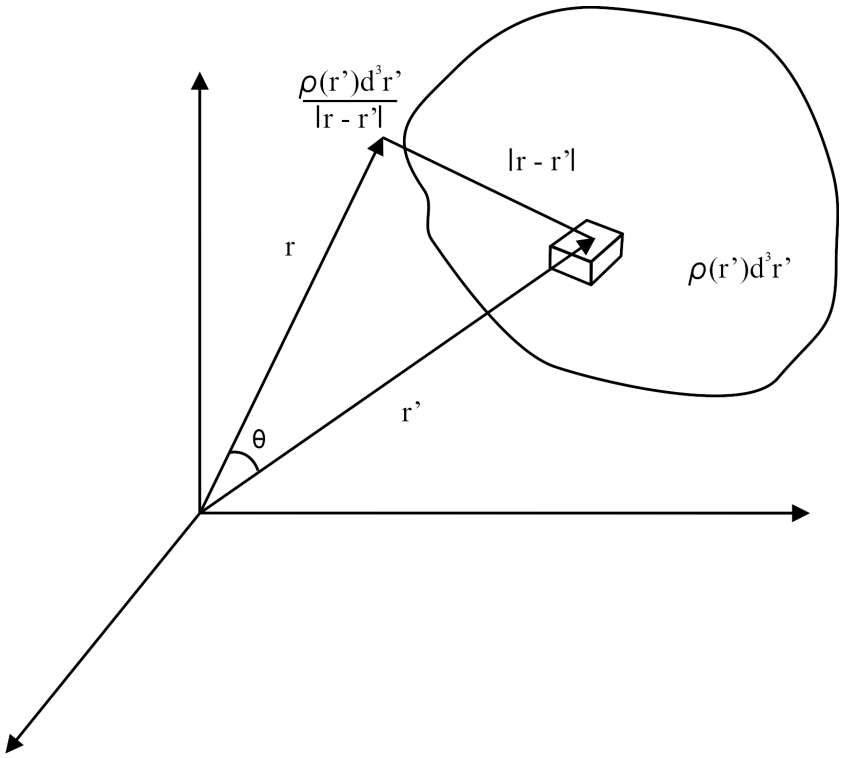

Electrostatic potential generated by a continuous charge distribution $\rho(\mathbf{r}')$. Potential generated at $\mathbf{r}$ is due to an infinitesimal charge $\rho(\mathbf{r}')\mathrm{d}^3r'$.

Source – Reference [3]

atoms in molecules, and it is clear that the choice is purely based on what is useful given a specific problem [27]. Other recent methods to determine $\rho(\mathbf{r})$ include a construction based on molecular fragments [19,20], multipole expansions centred on the nuclei [6,21–23] or distributed [15, 16, 24, 25], and also an expansion in spherical harmonics [7, 14, 26, 27].

No matter the method, what is noteworthy is that even the simplest one give a way to "discuss chemical effects, rationalise chemical reactivity or to search for empirical correlations between different types of experimental results" [26]. And of course, each method has specific regions and/or situations for which the method just is not suited.

5.1.1 MEP surfaces

There is another specific use of the MEP that is important for this work: the use of a MEP calculation in a region called the molecular surface. The molecular surface is a region which was proposed by Bader, in 1987 [31], as a good delimiter of molecular volumes. It is also called the $\rho(\mathbf{r}) = 0.001$ a.u. surface, and it contains roughly 97% of a molecule's electronic charge. MEP surfaces are used as a way to quantify intermolecular

interactions [34, 68], and it gives valuable indications as to which regions can interact with other molecules. Figure 1, repeated for convenience, shows an example MEP for $C_6H_3BrF_2$. Blue represent the most positive regions, and red the most negative, as it is shown in the scale ($kJ \cdot mol^{-1}$).

One of MEP surfaces problems appears when it is used to calculate surfaces for interacting molecules. When two molecules approach each other, the surfaces can "merge" in the region between the two, exactly the region of interest if ones wish is to analyse the interaction. An example of this problem is shown in a 2012 paper by Parker et al. [69], who calculated the effects of halogen bonding in the stabilisation of DNA molecules. Some of their calculations show the MEP surfaces merging in between the molecules. This is a region of importance to us, therefore novel methods to study intermolecular interactions are welcome, since by using MEP surfaces that region is not accessible.

Figure 1 - Example MEP surface of $C_6H_3BrF_2$

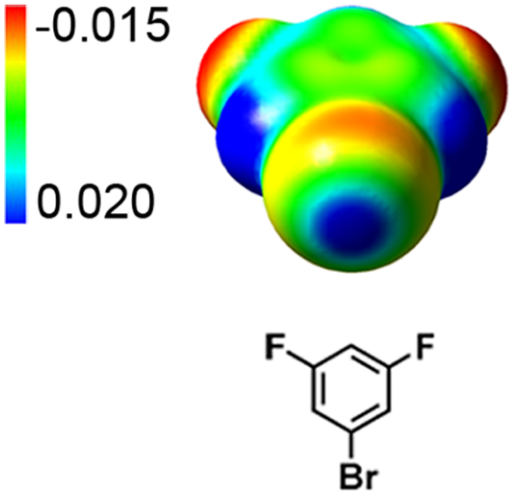

Source – Adapted from reference [32]

5.2 Developing the probe

5.2.1 Probe choice and calibration

As we have said at the beginning of this chapter, the probe needs to have a small dipole moment, to disturb the system as little as possible, and yet it has to be large enough for us to be able to study its effects on its neighbourhood. That makes polar molecules, like LiH or HF, bad candidates to be probes, since their dipole moment is too large compared with that of HD, which was our first candidate, with a dipole moment

Figure 4 – Dipole moment of the probe versus mass of the lighter particle.

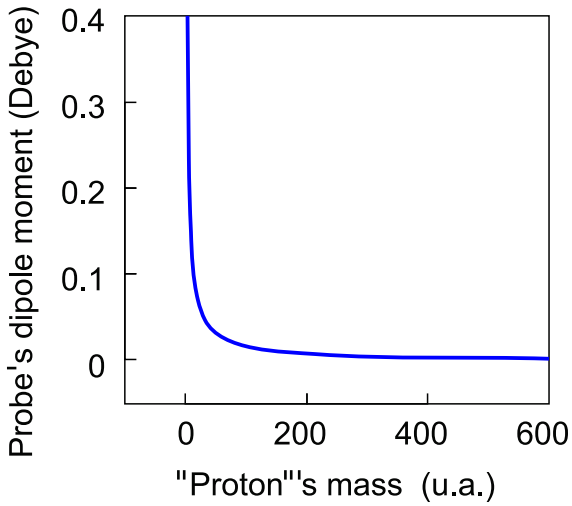

The graph displays the possible dipole moments for the probe when one of the atoms remains with the mass of the proton.

Source – The authors

of $\mu = 8.5 \times 10^{-4}$ debye[1]. However, that is too small for our objectives, and so we had to "construct" a virtual molecule to use in our quantum chemistry calculations. We need only to manipulate the probe's nuclear masses to amplify the isotopic effects on the dipole moment, and we have a good molecule to start our calibration.

We now have a two electrons and two protons probe, and the ability to alter nuclear masses in our calculations. The equilibrium distance of the probe is kept the same as H_2 equilibrium distance ($r_{eq} = 1.4$ a.u.) the reason for that will be explained in a later section. Figure 4 shows our study for the variation of the dipole moment of the probe with the change of mass. In this graph, one of the protons remains with its natural 1836.15 u.a. mass. As we can see, it is possible to produce large DM, compared to HD, if we use very small masses; the problem with that is that the adiabatic approximation is not valid for such small values of mass, so we have to take that in consideration. After some initial tests, we settled for masses M = 10000 a.u. and m = 50 a.u., for the heavy mass and the light one, respectively. This difference of mass is able to produce a dipole moment of $\mu = 0.086$ debye. This is two orders of magnitude larger than that of HD, and the three decimal figures remain the same even if we change computational methods (we used mainly configurations interactions and density functional theory throughout this work) and basis set. The choice of mass is a good compromise between having the largest isotopic dipole moment and maintaining adiabatic approximation valid for the probe.

The isotopic dipole moment points from M to m, because M is more effective in

[1] We chose the HD molecule as a starting point. It was the first candidate to be a valid probe, but this DM is very small, and FNMC is not very accurate for HD [49].

attracting electrons, so it corresponds to the negative region of a rigid dipole, as shown in Figure 5.

Figure 5 – The isotopic probe

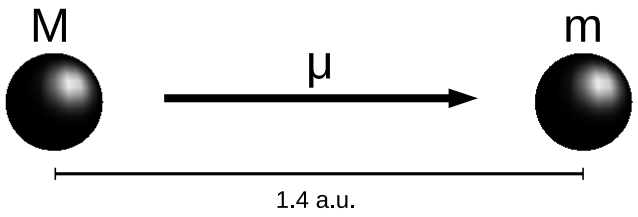

Source – The authors

5.2.2 Calculations of probe-molecule system energy with FNMC

Using the Hamiltonian operator for FNMC, equation (2.26), we can separate the energy of the probe-molecule system as

$$E = E_{BO} + E_{dm} = E_{BO} + E_{df} + E_{dp} + E_{d+m}, \tag{5.2}$$

being E_{BO} the BO energy of an equivalent calculation for the probe-molecule system, E_{dm} is the interaction energy of the probe dipole and the molecule, E_{df} is the energy of the dipole in the molecular electrostatic field, E_{dp} is the dipole-polarisation energy, and E_{d+m} is the constant FNMC contribution of the isolated molecule and probe. E_{BO} accounts for all lead, non-isotopic energy terms, so E_{dm} only has terms for the dipole interaction with the source molecule. Despite not being an issue, we do not neglect the positive constant term E_{d+m}, since the approach is not restricted to methods having size-consistency in FNMC calculations. On the other hand, for simplification purposes, whenever we refer to the isolation of a term in the right-hand side of equation (5.2), we will neglect E_{d+m}.

The probe-system energy interaction involves all classical and quantum contributions. Since we want to reduce this interaction to just the terms involving the isotopic dipole, we subtract the BO energy from equation (5.2). This is the reason why we chose to keep the equilibrium distance of the probe the same as that for H_2, for the consistency of this procedure. When we subtract E_{BO}, E_{dm} becomes

$$E_{dm} = E - E_{BO} = E_{df} + E_{dp} + E_{d+m} = -\mu\epsilon\cos\theta + E_{dp} + E_{d+m}, \tag{5.3}$$

in which θ is the angle between the electric field ϵ and the probe's dipole moment μ. The above equation allows us to identify two components of E_{dm}, which we can use to fit the data: the first term is the dipole field energy, and the second term is the energy due to

the polarisation of the molecule by the probe, E_{dp}. In some situations, explained in a later chapter, we found out that we can use the following classical formula for E_{dp}:

$$E_{dp} = -\frac{\alpha\mu^2(3\cos^2\theta + 1)}{2r^6}, \tag{5.4}$$

in which α is the isotropic polarisability.

Then, after we isolate E_{df}, we can obtain the electric field via the following equation:

$$\epsilon = \frac{\delta(E_{df})_{0\to\pi}}{2\mu}, \tag{5.5}$$

that is, the electric field is the difference of energy when the probe is parallel and anti-parallel with the field, divided by two times the moment of dipole of the probe. Another way of looking at this is, if the probe rotates in space, the plot of the angle of the probe relative to an arbitrary axis versus the energy of the system would be sinusoidal. In practice, this is how we programmed the probe. As exemplified in Figure 6, we place the probe in a point in space, and rotate it, in order to analyse the sinusoidal energy spectrum that we acquire as a result of the calculations. All calculations in this chapter were performed with CI/cc-pcVDZ.

Figure 6 – The isotopic probe between molecules

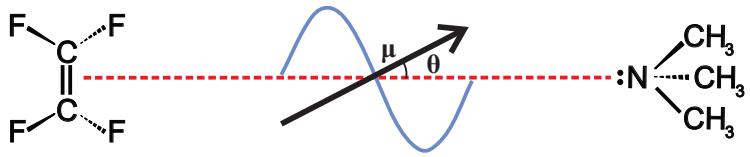

Source – The authors

5.2.3 The probe's rotation in space: a computational explanation

We will briefly explain how we actually use scripts to rotate the probe and perform single point energy calculations.

In general we only know the atom's positions described by an xyz file, which is a Cartesian description of the molecule, or system of molecules. We choose the point where the electric field will be evaluated to be the center of the probe. We have to calculate BO and FNMC energies. Using BO, the probe is simply a hydrogen molecule, since both atoms have infinite mass. We rotate the probe in both sets of calculations around its geometric centre.

The easiest way we found to calculate the electric field is to rotate the probe in three planes [2], the xy plane, the xz plane, and the yz plane. For each one we define an angle variable, which starts at zero, and variables for the atom's positions. The code below shows the declarations for xy plane: x1 and y1 are the two coordinates for the first atom, and x2 and y2 are the coordinates for the second atom. The probe is already included in the molecular Cartesian file, but with generic positions X1 Y1 Z1, X2 Y2 Z2. We then make a copy of the molecule's file and use the sed command to change the parameters directly in the file in order to request the calculation.

```
x1=0
y1=0
x2=0
y2=0
z1=0
z2=0
a=`echo "(${b}/10)*4*a(1)/180" | bc -l | awk '{printf "%3.9f", $0}'`
x1=`echo "(${cx}+(0.4*c(${a})))" | bc -l | awk '{printf "%3.9f", $0}'`
y1=`echo "(${cy}+(0.4*s(${a})))" | bc -l | awk '{printf "%3.9f", $0}'`
x2=`echo "2*(${cx})-(${x1})" | bc -l | awk '{printf "%3.9f", $0}'`
y2=`echo "2*(${cy})-(${y1})" | bc -l | awk '{printf "%3.9f", $0}'`
cp molecule.mol system.mol
sed -i -e "s/X1/${x1}/" system.mol
sed -i -e "s/Y1/${y1}/" system.mol
sed -i -e "s/X2/${x2}/" system.mol
sed -i -e "s/Y2/${y2}/" system.mol
sed -i -e "s/Z1/${cz}/" system.mol
sed -i -e "s/Z2/${cz}/" system.mol
```

This is repeated for both xz and yz planes. Each of the planes let us calculate two electric field vector's components. We perform BO and FNMC energy calculations, and then we subtract the first from the second. This subtraction generates three data sets, xy, xz and yz.

```
dalton -N 6 fnmc.dal system.mol
En=`cat fnmc_system.out | awk '{if ($1=="Total" && $2=="energy") print
    $3 }'`
echo "${a} ${En}" >> FNMCxz
dalton -N 6 bo.dal system.mol
Enbo=`cat bo_system.out | awk '{if ($1=="Total" && $2=="energy") print
    $3 }'`
echo "${a} ${Enbo}" >> BOxz
```

[2] Although we think it is possible to perform the probe's rotation with spherical coordinates, making one data set instead of three, it is beyond our programming abilities at this point in time.

```
7 b=`echo "${b} + 360" | bc `
```

For each data set we fit the sinusoidal function (5.3), and from the fit we capture the amplitude of the cosine function, and a phase angle. This phase angle exists because the electric field's direction is not known *a priori*. The probe starts in the direction of one of the axis (the first letter on the data set name), and we calculate the first energy value. After this calculation, we capture the energy for the configuration, it generates new values for the probe's atom's position, based on a predetermined value, which is a step the angle gets every iteration. The code loops until the probe's rotation is complete.

We fit the data using the following equation:

$$f(x) = a\cos(x - b) + c, \tag{5.6}$$

and with the adjusted parameters for the three data sets, we can calculate the electric field using a simple equation of this type:

$$\epsilon = \sqrt{\left(\frac{a_{xy}}{\mu}\cos b_{xy}\right)^2 + \left(\frac{a_{xy}}{\mu}\sin b_{xy}\right)^2 + \left(\frac{a_{xz}}{\mu}\sin b_{xz}\right)^2}. \tag{5.7}$$

a_{xy}, a_{xz}, b_{xy}, and b_{xz} are the adjusted parameters of equation (5.6), the indices show to which data set they belong. The fit is done with GNUPLOT's implementation of the nonlinear least-squares (NLLS) Marquardt-Levenberg algorithm [70].

This procedure is enough to calculate the electric field. There are some cases where we would not have an electric field in the region, and in those cases we would fit the data sets with an equation like the following:

$$f(x) = a(3\cos x^2 + 1) + b, \tag{5.8}$$

which is an implementation of equation (5.4).

The most general case, in which both E_{dp} and E_{df} are important, we would fit both functions together to analyse. The study of E_{dp} via this method is still on its early stages, as we are not sure that the classical equation can be used to analyse molecular systems in every scenario.

5.3 Tests with H_2, H_2O, benzene and chlorobenzene

Having determined the method of analysis, the next step is to perform tests with simple systems to gauge the performance of the probe. All of our calculations were done with either GAMESS [54] or Dalton [52, 53] programs.

First test was done with an H_2 molecule, that has no permanent dipole moment, so the interaction of the probe and the molecule is lead by its quadrupole moment. There

were three tests, all shown in figure 7. The first one was to check the behaviour when the probe distances itself from the molecule, with a fixed angle. The data is shown as triangles in the graph, with the green line representing the fit of an r^{-4} function that was done from r = 8 a.u.. So, if the probe is far from the molecule, we see its interaction mainly with the quadrupole moment, and when it is near, we see that the interaction gets more complicated, and the polarisation term, r^{-6}, is the leading dependence in the energy in that region.

Then we fixed the probe-molecule distance as 5 a.u. and rotated the probe. E_{dm} for that calculation is in inset (a). This is very close to what we would expect from a classical dipole-polarisability interaction, equation (5.4), but it has other contributions, at least E_{df}. After that, we subtracted the polarisation contribution in E_{dm}, and obtained inset (b) in the graph, representing E_{df}. This quadrupole electric field was evaluated to be $\epsilon = 2.6 \times 10^{-4}$ a.u.. This is a very small electric field, and an indicative that we had developed a highly accurate method of analysis.

Figure 7 – Interaction of the probe with an H_2 molecule

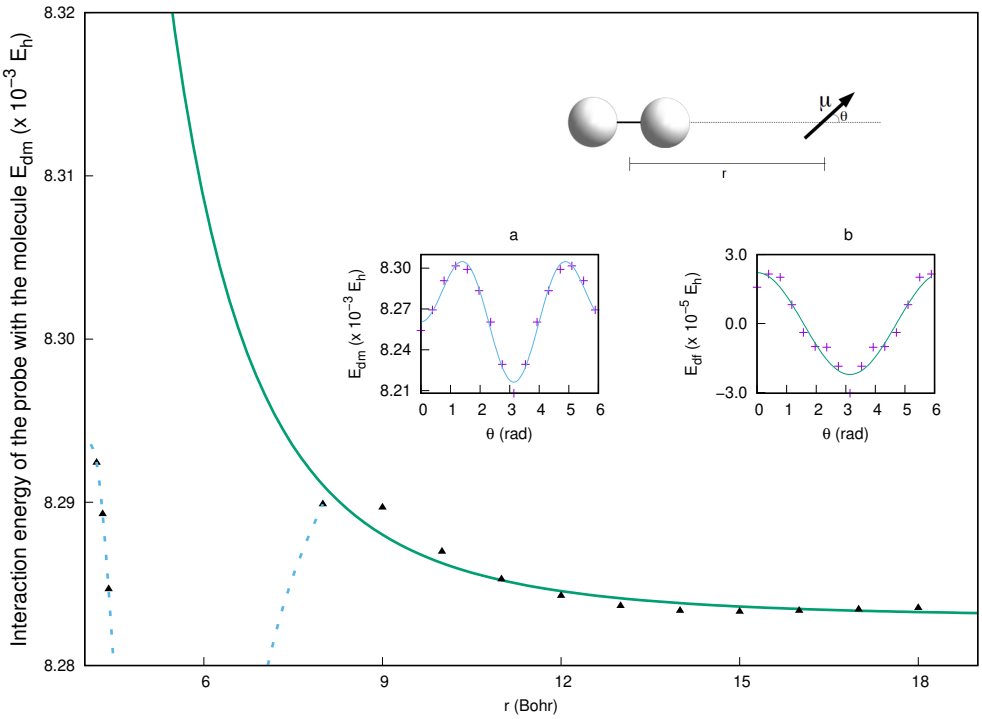

Energy of the probe's interaction with a molecule of H_2 along the axis of the molecule. Triangles correspond to calculated data, and the full line is an adjustment of an r^{-4} function from r = 8 a.u.. Inset (a) shows E_{dm} for r = 5 a.u. and inset (b) shows E_{df} for the probe-quadrupole interaction.

Source – The authors

The next test was performed with water, one of the most important molecules in our universe, constant target of both theoretical and experimental research. Although be-

ing widely studied, and having many models and computational methods, some of water's properties are yet to be determined with sufficient precision [71]. Beyond liquid phase, the study of water's crystallisation is important in climate research and has applications in diverse areas of engineering, i.e. aviation, transmission of electric energy, and eolic energy production [72]. Going even further, the study of non-crystalline states may help build a better understanding of water's liquid state [73–75].

Water is also the system of choice in the study of hydrogen bonds [76–78]. Understanding hydrogen bond is of universal importance: physicists, chemists, biologists and material scientists have being studying this kind of interaction for over a century, not just for the understanding of water and its clusters, but also the general formation of the interaction.

One of the first tests we did was to plot the electric field around a water dimer, shown in Figure 8. This image has no information about the field intensities, but it allows us to know that the probe was aligning correctly with the molecule's field.

Figure 8 – Electric field around a water dimer

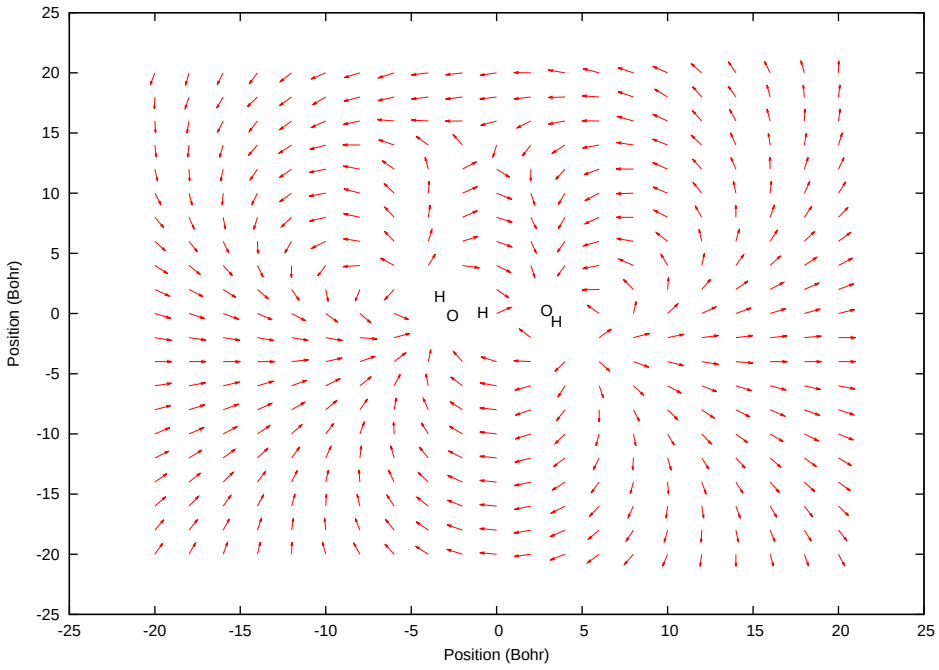

Image shows the direction of the electric field vector around a water dimer, in the plane of the left water molecule. In the second molecule, there is a hydrogen above the plane, and one below it, both at the same xy position.

Source – The authors

Further analysis of the electric field was done with an isolated water molecule. Since water is a highly polar molecule, the fit of E_{dm} to a pure cosine function is very accurate, because E_{df} is strongly dominant, as we can see in the results presented in

Figure 9. If we isolate E_{dp} for one of them, we see a different behaviour than what we've seen previously, depicted on the inset of figure 9. We assumed this is due to the oxygen's electron pairs, and maybe this might contribute to better understanding of hydrogen bonds. At this point we are not sure, but this deserves future investigation.

Figure 9 – Interaction of the probe with an H_2O molecule

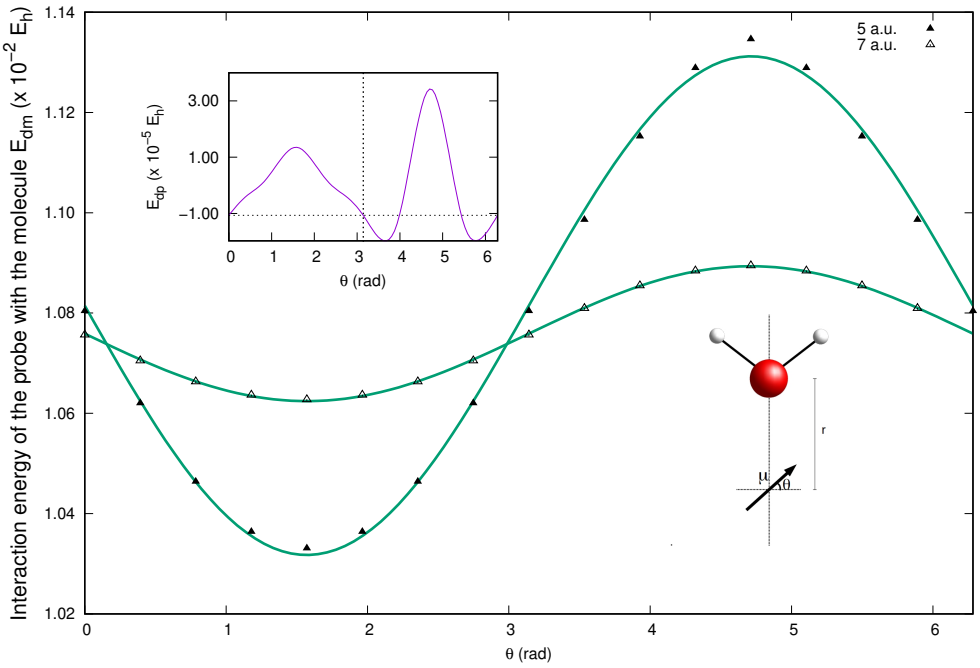

Energy of the probe's interaction with a water molecule along its symmetry axis and close to the O atom for two distances. The inset shows E_{dp} at r = 5 a.u..

Source – The authors

We then analysed two ring systems, benzene and chlorobenzene, both with the probe placed at the center of the ring. The difference between the two is that benzene does not have an electric field in its center, whereas chlorobenzene has.

Inside the benzene ring, the interaction is purely due to E_{dp}, but we cannot use the point approximation, since the probe is surrounded by the molecule. BO and FNMC show minima at the C-C bonds, as expected. E_{dm}, though, shows minima when the probe points to the C atoms, which are the polarisable centers for the molecule. Data is shown on Figure 10.

Besides, we also calculated the electric field on the axis perpendicular to the plane of the benzene molecule, with each hydrogen being replaced by deuteron atoms. Table 3 shows that the electric field decreases very slowly with each additional hydrogen replacement. The configuration represents the position of each H or D atoms, H being shown as 1, and D as 2. These electric fields are very small, smaller than our error margin, but the

Figure 10 – Interaction of the probe with a benzene molecule

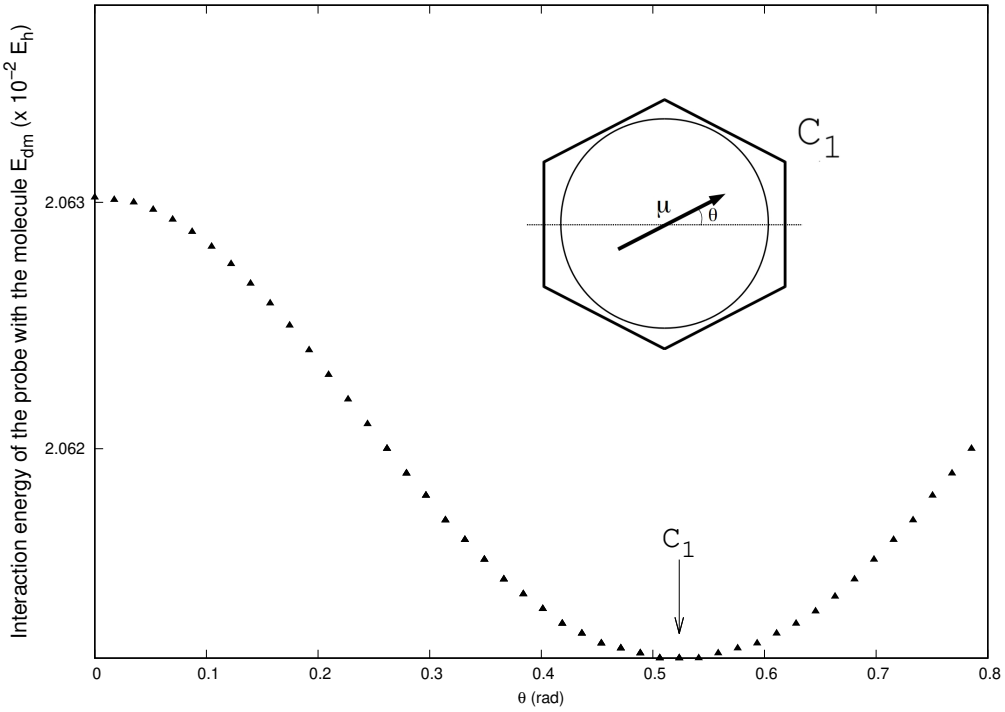

Energy of the probe's interaction with a benzene molecule. Probe is located at the center of the ring, identifying the C_1 carbon atom.

Source – The authors

result is systematic, and gave us better understanding of the capabilities of the probe as an electric field evaluator.

On the other hand, chlorobenzene has an electric field at its center. We see the fitted data in Figure 11. We used the point approximation in this case, considering the chlorine atom as a point particle. The inset of figure 11 shows E_{df} for this system, acquired after the subtraction of the classical E_{dp}. We evaluated the electric field as $\epsilon = 5.3 \times 10^{-3}$ a.u., pointing at the chlorine atom.

The use of the probe to analyse molecular environments represents a change in paradigm compared with the use of the MEP and other methods. The probe works well in many different environments, and can be used to evaluate electric fields and to identify polarisable, possibly reactive, sites in molecules.

Table 3 – Electric field of benzene with isotopic substitutions.

Configuration	Electric Field (a.u.)
111111	0.033979
211111	0.034082
221111	0.034080
212111	0.034080
211211	0.034081
222111	0.034077
221211	0.034077
212121	0.034077
222211	0.034076
222121	0.034076
221221	0.034076
122222	0.033967
222222	0.034070

Source – The authors.

Electric field of benzene with isotopic substitutions. Configuration column shows the position of hydrogen (1) and/or deuteron (2) atoms.

Figure 11 – Interaction of the probe with a chlorobenzene molecule

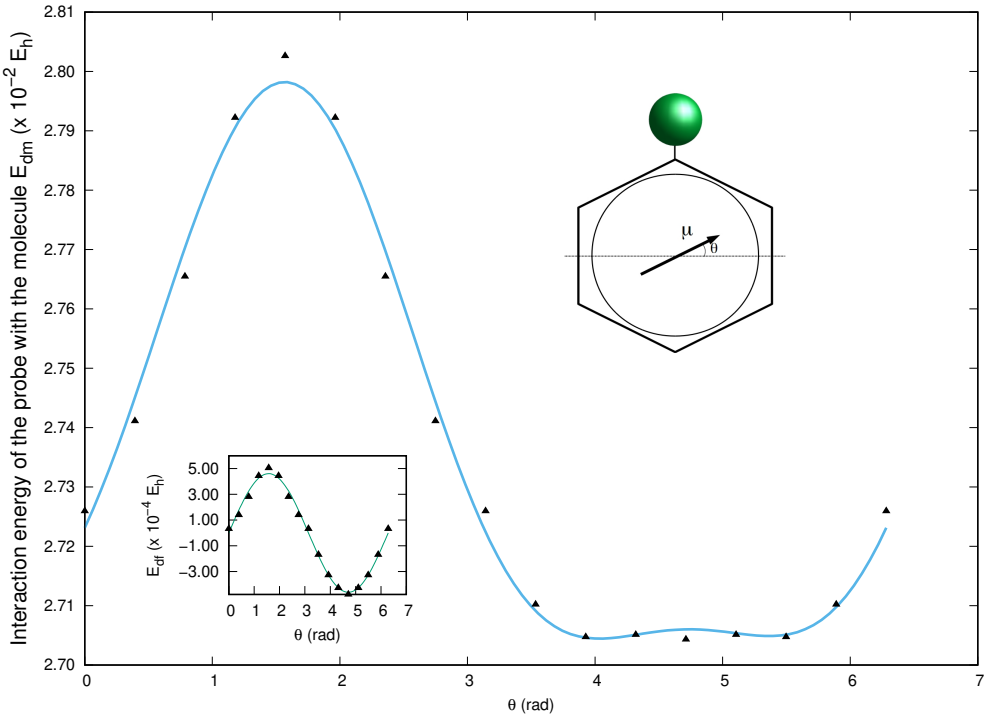

Energy of the probe's interaction with a chlorobenzene molecule. Probe is at the center of the ring. Inset shows E_{df}.

Source – The authors

6 Applying the method

Having calibrated the probe, and knowing well what it could do, we started searching for systems of interest in which we could utilise the method. Firs of them, published together with the method in [79] was a problem associated with the electric field inside the phosphine-borane frustrated Lewis pair (FLP).

6.1 Phosphime-borane FLP

6.1.1 Lewis pair

Lewis' pairs, proposed by G. N. Lewis in 1923 [80], are molecule pairs, one being an electron donor (Lewis' base) and the other one being an electron receptor (Lewis' acid). This concept is central to the understanding of a large part of the chemistry of the principal group and the chemistry of transition metals. This proposition was an attempt to break the line of thought that Lewis called "cult of the proton", in which only proton donors were considered as acids.

This new acid-base notion was used to understand many reactions. A classic example is the system $NH_3 \cdot BCl_3$, shown in Figure 12. The system is neutralised, similarly to what happens to a Brønsted acid-base pair, but it doesn't generate water, the result is an adduct.

Figure 12 – $NH_3 \cdot BCl_3$ Lewis pair.

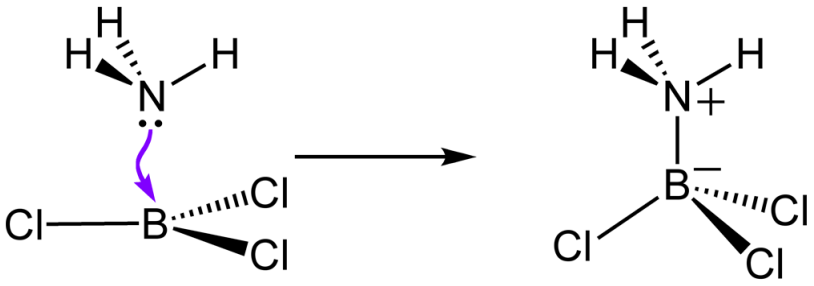

$NH_3 \cdot BCl_3$ Lewis pair. NH_3 is a Lewis base, and BCl_3 is a Lewis acid. The pair reacts and forms an adduct.

Source – Adapted from Wikipedia [81].

6.1.2 Frustrated Lewis pairs

FLP are compounds containing a Lewis acid and a Lewis base that cannot form an adduct because of steric hindrance, caused by its large substituents [82,83], as can be seen in figure 13. FLP have great importance for fundamental transformation processes and also for biological functions.

Figure 13 – FLP $(C_6F_5)_3B - P(tBu)_3$.

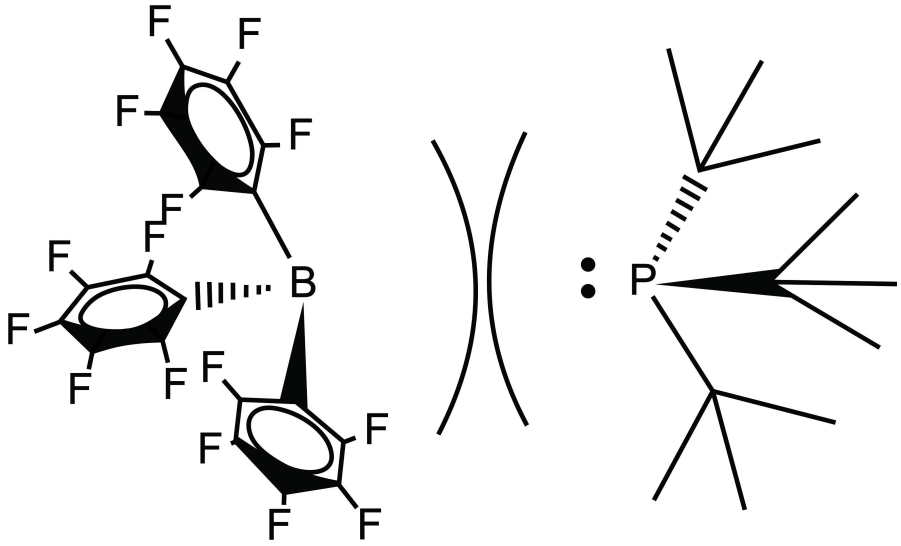

FLP $(C_6F_5)_3B - P(tBu)_3$. Hindrance caused by large substituents makes it impossible the formation of an adduct.

Source – Adapted from [84]

One of the most important uses of FLP is hydrogen activation [85]. Transition metal systems are known by their ability to free or react with H_2, but non-metallic systems that do the same are rare. Some of those compounds were studied by Welch et al. [86,87], even before the term FLP was proposed by Stephan, in 2008 [82].

Since then, many research groups have worked to understand this hydrogen activation reaction mechanism by FLP [88–94], and also the reason for some FLP not to perform the same reaction with H_2 [95]. Two different mechanisms were proposed for this activation. One was an electron transfer mechanism, indicating the activation of the molecule by a complex electron transfer between the FLP and the hydrogen. The other one, which we tested, was the activation of the hydrogen molecule solely because of the electric field inside the FLP.

The first method to verify if the activation occurs because of FLP's electric field [88, 89] does not consider the FLP explicitly, but calculates the required electric field to activate an H_2 molecule, and conjectures that it would be the electric field inside the FLP. According to this model, the electric field should be larger than 0.1 u.a.. The

distance between the phosphorus and the boron atoms is very large, 7.9 u.a., so this would be a huge electric field inside the FLP's "cavity". The other method devised to explain this phenomenon was a complex and dynamic electron transfer mechanism [93, 94, 96]. Simulations helped this electron transfer method by including transition states.

DFT MEP calculations evaluated the electric field inside the FLP as between 0.08 u.a. and 0.1 u.a. [90], but according to the literature, this method fails near phosphorus atoms, overestimates charge polarity, exaggerates correlation effects between electrons, and does not have better performance than HF MEP [3, 97, 98]. Therefore, checking the EF inside the FLP becomes a good application of the isotopic probe.

Figure 14 – Probing points and results for the FLP.

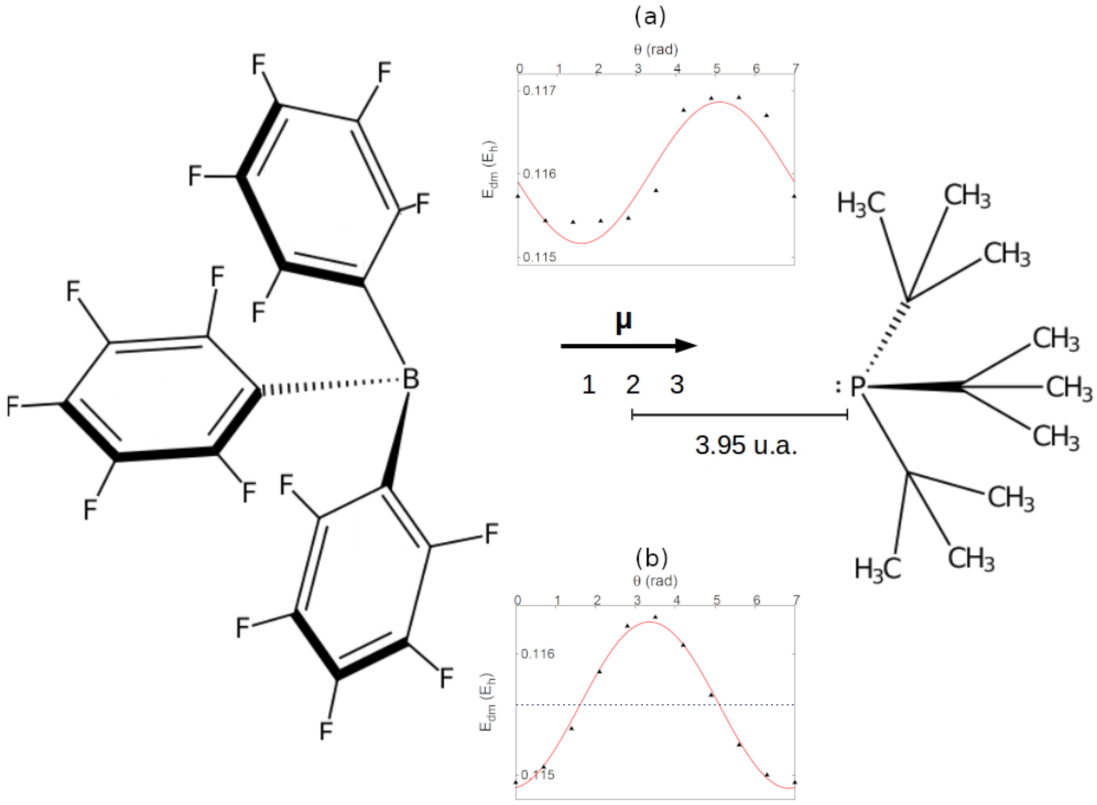

Probing of the FLP's cavity. Distances 1-2 and 2-3 are 0.44 a.u.. Inset (A) shows E_{dm} for Rokob's geometry of the FLP [90]. Inset (B) shows calculations in the TS1 state from Liu [93].

Source – The authors

This was our first system analysed using DFT[1]. The number of electrons was too big for us to use CI with our available computers. Electric field was calculated in three

[1] Cartesian coordinates for the systems are on appendix A, Tables 13 and 14

regions, points 1, 2 and 3, shown in Figure 14, and were evaluated as $\epsilon_1 = 0.009$ a.u., $\epsilon_2 = 0.013$ a.u., $\epsilon_3 = 0.021$ a.u. as shown in Table 4. This means that our results did not support the assumption of the electric field model, but they seem to agree with the electron transfer model for the hydrogen activation by a phosphine-borane FLP, also reported in [79]. Inset (a) of Figure 14 shows E_{dm} for one of those calculations. Inset (b) shows E_{dm} of a calculation for the electric field from the TS1 configuration reported by Liu [93]. This configuration shows practically no E_{dp} contribution, and that shows us that the electric field there is purely electrostatic. This result is consistent with the displacement of the FLP electron pair in TS1, which makes E_{dp} negligible.

Table 4 – Electric field inside the FLP's cavity.

System	Position	Electric Field (a.u.)
FLP	1	0.009
	2	0.013
	3	0.021

Source – The authors.

Electric field inside the FLP's cavity. Positions shown are the ones depicted in Figure 14.

6.2 Probing of intermolecular interactions: π- and σ-holes

Another application we've found for the probe is the study of intermolecular interactions. The probe is small, having 1.4 a.u. of internuclear distance, but its actual size is larger because we have to account for its electron cloud volume. Most intermolecular distances are about 5.7 a.u..

Intermolecular interactions are assumed to be fully described as Coulombian interactions, i.e. electrostatic plus polarisation [33–35]. This is why we can use the MEPS in order to study them [68]. As we explained in chapter 5, MEPS are maps of the electrostatic potential around the molecule, taken over a region defined as the surface of the molecule [31], and it is one of the main techniques used to analyse intermolecular interactions.

However, we have already shown that MEPS is not appropriate to study the kind of bonds we are concerned here, as it does not have good resolution in said regions. In consequence, we now use the isotopic probe to analyse several intermolecular interactions of molecules containing π- and/or σ-holes. Based on the Hellmann-Feynmann theorem [56, 99], which states that intermolecular forces are all electrostatic in nature, we propose the electric field as a quantifier for the intermolecular bonds.

6.2.1 π- and σ-holes

Both π and σ holes are non-nuclear molecular regions of positive electric potential that interact with negative regions, e.g. electron pairs of other molecules like H_2O or NH_3.

σ-holes are extensions of sigma bonds. Covalent bonds can be amphoteric and cause an outer atom to have both positive and negative surface potential, for example a halogen that has his electron cloud disposed in a ring with radius perpendicular to the bond [100]. This phenomenon makes it so that the atom, although having high electronegativity, can have a positive electrostatic potential opposite to its covalent bond that can interact with negative sites. This region of positive electrostatic potential is called a σ-hole. Specifically, if the atom is an halogen, the bond created by this type of interaction is called a halogen bond. A σ-hole interaction is very similar to a hydrogen bond: both are highly linear (hydrogen bonds are slightly less linear than halogen bonds [33]) and have similar strength. They can even compete in some situations, showing a potential for the design of biological macromolecules [101].

π-holes, on the other hand, are regions more central to the molecule that happen when a group of outer atoms are more electronegative than the central atoms, so that they attract the electrons to the edges of the molecule, leaving behind a positive center, a "hole" in the electron cloud, that we call a π-hole. One of the earlier theoretical and experimental studies on π-holes was only a few decades ago by Alkorta [102, 103], who compared the differences between C_6F_6 and benzene, C_6H_6. He concluded that the fluorine atoms invert the electron-donor characteristics of the carbon atoms. Most of the studies that followed showed the importance of the π-hole lone pair interaction, with oxygen being the electron donor, certainly because of the importance to understand biochemically this interaction, since water is the most important molecule for life [104, 105]. Many more studies were carried on the topic; to cite a few, there are articles showing lone pair - π-hole interactions in synthetic molecules [106], competition between π-hole and σ-hole interactions on the same molecule [107], intramolecular π-hole bonds [108], cooperation of non-covalent bonds [76], π-hole - water interactions [109], and estimating that these bonds can be as strong as hydrogen bonds [110].

In order to verify this last statement, we calculated the electric field in the middle of a hydrogen bond between two ammonia molecules, to compare with the other kinds of interaction. All the calculations for these interactions were performed with DFT, using 6-31G** basis and three different functionals: B97-D, PBE0-D3 and B3LYP-D3. The D3 in PBE0 and B3LYP stands for Grimme's DFT-D3 correction for dispersion interactions [111]. The probe was always placed in the midpoint of the interaction, unless stated otherwise.

The geometry that we used for the ammonia dimer was optimised by Jurecka et

al. [112][2]. For the ammonia dimer, Figure 15, with R_{eq}= 4.72 a.u. a proper sinusoidal fit was found, so that the EF could be evaluated and used as a basis of comparison between a hydrogen bond and the π and σ-hole bonds. As we mentioned at the start of this section, we expected the hydrogen bond to be similar in strength to σ-holes, and perhaps to some of the π-holes. The results of the electric field calculations are contained in Table 5. Different DFT functionals generated a very good accordance with the larger difference being about 7%. The average electric field among the functionals was 0.1 a.u., which is a very large electric field. Recall that the field needed to separate a hydrogen molecule is about 0.1 a.u..

Figure 15 – E_{dm} of the hydrogen bond between two ammonia molecules.

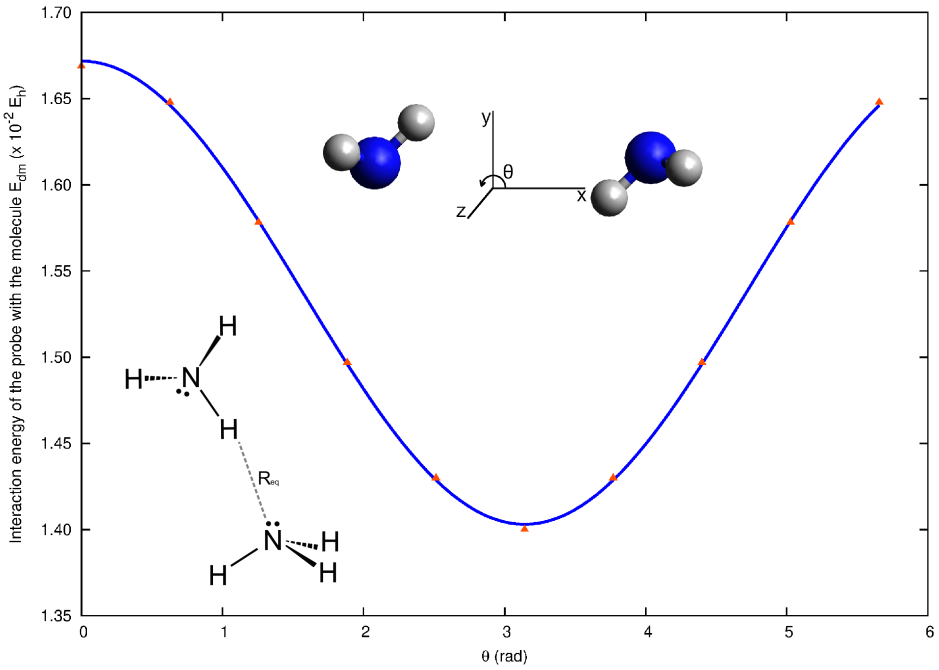

Hydrogen bond between two ammonia molecules. Triangles are the calculated E_{dm} values from the xy data set, while the line is the fit to the best sinusoidal curve used to evaluate the electrostatic field

Source – The authors

All the systems whose interactions were analysed are listed in Table 6. Those systems have been experimentally characterised, and their π- and σ-holes have been properly identified. The Table also shows their equilibrium distance and energy, calculated using DFT/B3LYP-D3.

We started studying the interactions of the $C_6F_6 \cdots H_2O$ system, which were experimentally characterised by [109], who used infrared spectroscopy and also optimised the geometries with B3LYP/aug-cc-pVTZ calculations. They encountered three configu-

[2] Cartesian coordinates for the system are on appendix A, Table 15.

Table 5 – Electric field in the hydrogen bond between two ammonia molecules.

System	Functional	Bond EF (a.u.)
Ammonia dimer ($2NH_3$)	B97-D	0.11
	PBE0-D3	0.12
	B3LYP-D3	0.12

Source – The authors

Table 6 – Equilibrium distances and energies for analysed systems.

System	R_{eq} (a.u.)	Energy (E_h)
NH_3 dimer	4.724	-113.04919
C_2F_4 and TMI	5.575	-649.69735
C_2F_3Cl and TMI - π	5.518	-1010.03062
C_2F_3Cl and TMI - σ	5.631	-824.43113
C_2F_3Br and TMI - π	5.518	-3123.91052
C_2F_3Br and TMI - σ	5.386	-3123.91178
C_6F_6 and water - Above the center	6.198	-903.73291
C_6F_6 and water - Above the bond	6.085	-903.65368
C_6F_6 and water - Above the atom	5.348	-903.64397
C_6Cl_6 and water - Above the center	5.726	-3065.66083
C_6Br_6 and water - Above the center	5.820	-15748.93034

Source – The authors

Equilibrium distances (R_{eq}) and energies of the analysed systems, calculated with B3LYP-D3/6-31G**.

rations for the system, that we will call "above the center", "above the bond" and "above the atom", following Wang's nomenclature [32]. The three configurations can be seen in Figure 16[3]. In the "above the center" configuration, calculations show no electric field in planes parallel to the ring; as expected, the electric field for this configuration is in the direction of the ring's axis. This first configuration shows the larger electric field of the three shown in Figure 16, being slightly larger than that of the ammonia dimer. We can see the results in Table 7. Figure 17 shows E_{dm} calculations for one of the data sets of the "above the center" configuration.

We have calculated the bond electric fields at the midpoint of the dashed lines in Figure 16, this is what we call the *midpoint of the interaction*. For the "above the center" structure, we can justify that the bond should be in that direction, but, for the other two, it is possible that there were other points of interest for the interaction. However, we decided to restrict the calculations to the smaller distance between the two molecules. For instance, the "above the atom" structure has the water molecule rotated in a way

[3] Cartesian coordinates can be seen in Tables 16, 17 and 18, on appendix A.

Figure 16 – $C_6F_6 \cdots H_2O$ configurations.

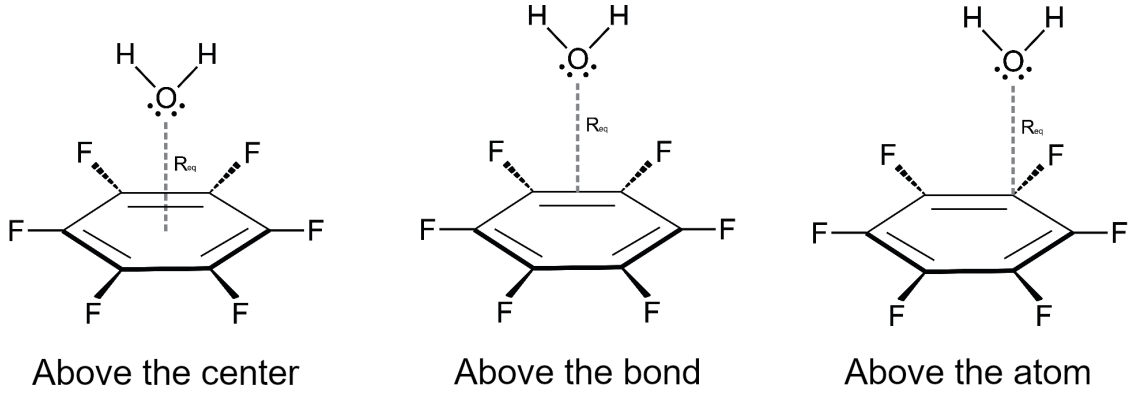

The three configurations for $C_6F_6 \cdots H_2O$ reported by Amicangelo [109], and whose bond electric field were studied during this work.

Source – The authors

that the oxygen's pairs of electrons face the center of the ring, and one of the hydrogen atoms is closer to a fluorine atom. It is possible that the bond is not along the shorter O-C distance, but actually occurs in the O-center direction and simultaneously in the H-F direction. That being said, we do not think the determination of a "bond direction" is a simple matter. As we interpret it, the whole molecule is responsible for the bond, and by analysing the electric field in the region where they are closer together we can better understand the interaction.

Table 7 – Electric fields in the π-hole interaction of $C_6F_6 \cdots H_2O$.

C_6F_6 and water	Functional	Bond EF (a.u.)
Above the center	B97-D	0.14
	PBE0-D3	0.15
	B3LYP-D3	0.14
Above the bond	B97-D	0.05
	PBE0-D3	0.06
	B3LYP-D3	0.06
Above the atom	B97-D	0.07
	PBE0-D3	0.08
	B3LYP-D3	0.08

Source – The authors

Electric field in the π-hole interaction of the $C_6F_6 \cdots H_2O$ system for the different functionals.

We have also calculated the electric field of $C_6Cl_6 \cdots H_2O$ and $C_6Br_6 \cdots H_2O$, both in the "above the center" configuration. Wang et al. [32] have proposed that, for cyclic systems, the π-hole strength is proportional to the strength of the electron-withdrawing

Figure 17 – E_{dm} of $C_6F_6 \cdots H_2O$.

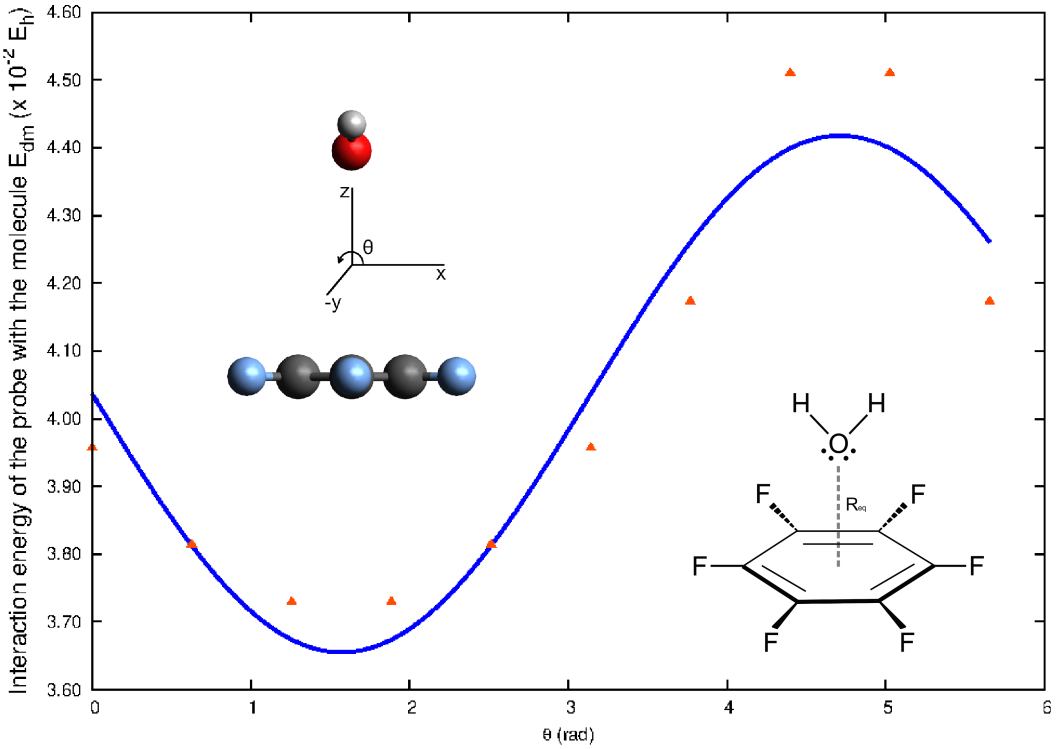

Calculation of E_{dm} for the $C_6F_6 \cdots H_2O$ system, "above the center" configuration, as shown in the image. Energies are calculated in the midpoint of the interaction. Triangles are the calculated energies of the xz data set, and the line is the sinusoidal fit of equation (5.3).

Source – The authors

substituent groups, in this case, the electronegativity of the outer atoms. This proposition matches our results, shown in Table 8, which is an indicative that the electric field can be used as a quantifier for the bonds.

π-hole interactions are not exclusive to cyclic molecules though, and we've analysed some open chain molecules that also show π-holes. C_2F_3X (X=F,Cl,Br) were experimentally characterised with infrared and Raman spectroscopy by Geboes et al. [113] while interacting with trimethylamine (TMA, C_3H_9N). Some of these molecules also show σ-holes and interact via this region with TMA, but we will start the analysis with the π-hole compounds. Figures 18, 19 and 20 show E_{dm} for the $C_2F_4 \cdots$ TMA, $C_2F_3Cl \cdots$ TMA and $C_2F_3Br \cdots$ TMA systems, respectively[4].

Contrary to what we have seen for the cyclic systems, these systems do not show correlations based on the electronegativity of the substituents. The electric fields of the systems are shown in Table 9. We can see that the electric field drops to about half of the value of the ones generated by the cyclic complexes. The correlation described by

[4] Cartesian coordinates for the systems are on appendix A, Tables 19, 20 and 21

Table 8 – Electric fields in the π-hole interaction of $C_6X_6 \cdots H_2O$.

C_6F_6 and water	Functional	Bond EF (a.u.)
C_6F_6 and water	B97-D	0.14
	PBE0-D3	0.15
	B3LYP-D3	0.14
C_6Cl_6 and water	B97-D	0.12
	PBE0-D3	0.13
	B3LYP-D3	0.13
C_6Br_6 and water	B97-D	0.11
	PBE0-D3	0.13
	B3LYP-D3	0.12

Source – The authors

Electric field in the π-hole interaction of the $C_6X_6 \cdots H_2O$, (X = F, Cl, Br) systems for the different functionals, on the "above the center" configuration.

Figure 18 – E_{dm} of $C_2F_4 \cdots$ TMA.

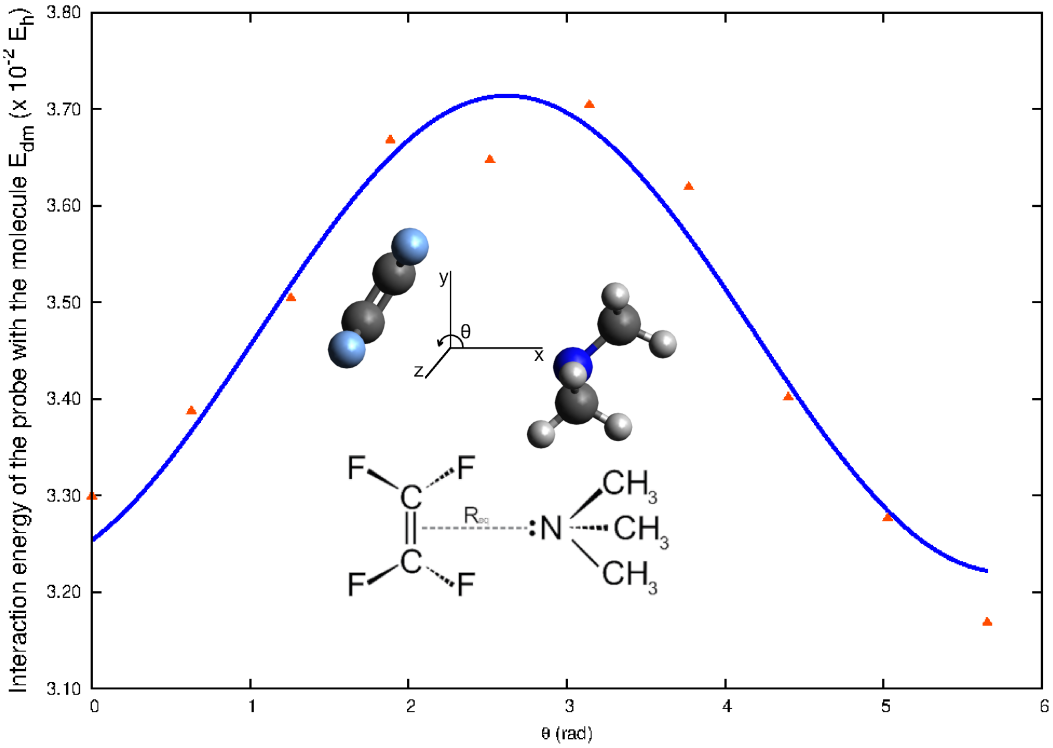

E_{dm} calculation for the $C_2F_4 \cdots$ TMA system, as shown in the image. Energies are calculated in the midpoint of the interaction. Triangles are the calculated energies of the xy data set, and the line is the sinusoidal fit of equation (5.3).

Source – The authors

Figure 19 – E_{dm} of π-bonded $C_2F_3Cl \cdots TMA$.

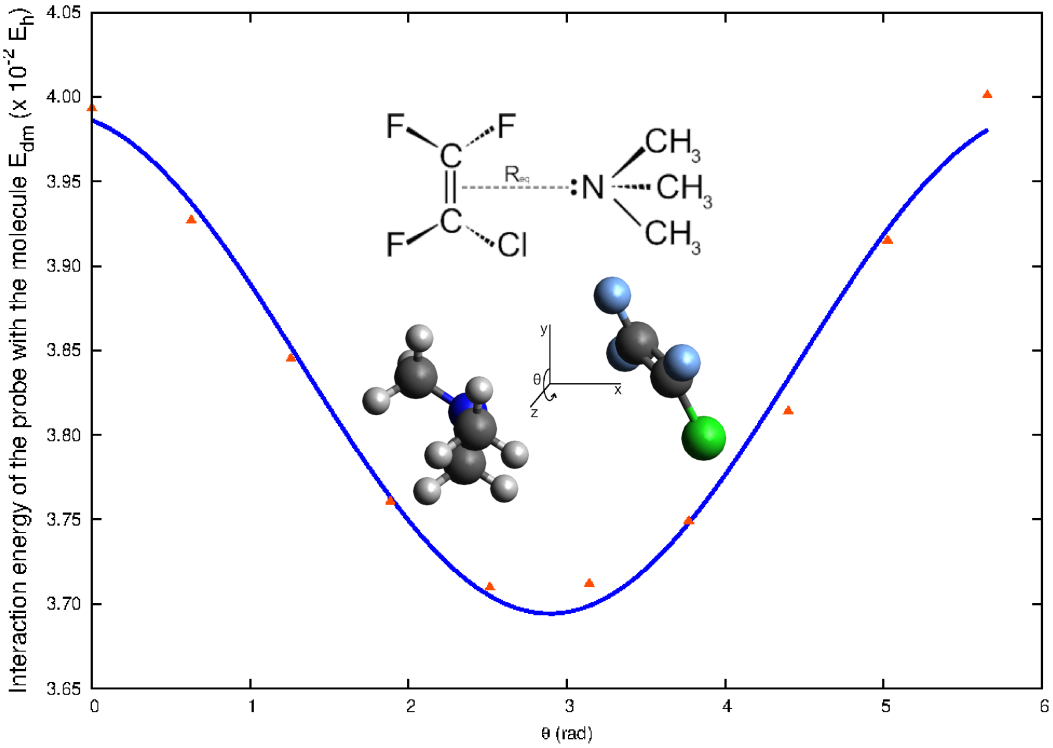

E_{dm} calculation for the $C_2F_3Cl \cdots TMA$ system, as shown in the image. Energies are calculated in the midpoint of the interaction. Triangles are the calculated energies of the yz data set, and the line is the sinusoidal fit of equation (5.3).

Source – The authors

Wang et al. is not present: in this case, the electric field increases with the inverse of the electronegativity.

Table 9 – Electric fields in the π-hole interaction of $C_2F_3X \cdots TMA$.

C_6F_6 and water	Functional	Bond EF (a.u.)
C_2F_4 and TMA	B97-D	0.06
	PBE0-D3	0.07
	B3LYP-D3	0.07
C_2F_3Cl and TMA	B97-D	0.07
	PBE0-D3	0.08
	B3LYP-D3	0.08
C_2F_3Br and TMA	B97-D	0.06
	PBE0-D3	0.07
	B3LYP-D3	0.07

Source – The authors

Electric field in the π-hole interaction of the $C_2F_3X \cdots TMA$ (X = F, Cl, Br) systems for the different functionals.

Figure 20 – E_{dm} of π-bonded $C_2F_3Br\cdots TMA$.

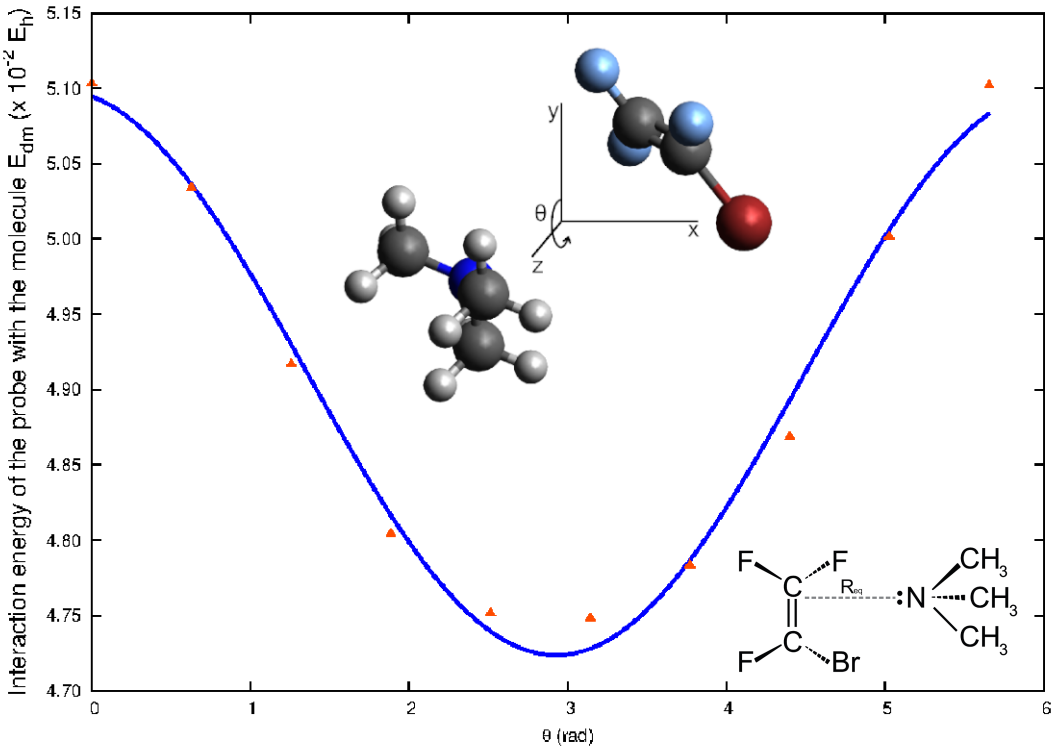

E_{dm} calculation for the $C_2F_3Br\cdots TMA$ system, as shown in the image. Energies are calculated in the midpoint of the interaction. Triangles are the calculated energies of the yz data set, and the line is the sinusoidal fit of equation (5.3).

Source – The authors

Finally, we studied the σ-hole bonded systems: $C_2F_3Cl\cdots TMA$ and $C_2F_3Br\cdots TMA$[5], with results shown in Table 10[6].

Table 10 – Electric fields in the σ-hole interaction of $C_2F_3X\cdots TMA$.

C_6F_3X and TMA	Functional	Bond EF (a.u.)
	B97-D	0.07
C_2F_3Cl and TMA	PBE0-D3	0.08
	B3LYP-D3	0.08
	B97-D	0.09
C_2F_3Br and TMA	PBE0-D3	0.10
	B3LYP-D3	0.11

Source – The authors

Electric field in the σ-hole interaction of the $C_2F_3X\cdots TMA$ (X = Cl, Br) systems for the different functionals.

[5] C_2F_4 does not present a σ-hole.
[6] Cartesian coordinates for the systems are on appendix A, Tables 22 and 23

In the case of these σ-hole bonded complexes, our results are, again, in accordance with Wang's proposition that the strength of the σ-hole is proportional to the size of the atom. Figures 21 and 22 show the sinusoidal fit for one of the data sets of both systems.

Figure 21 – E_{dm} of σ-bonded $C_2F_3Cl\cdots TMA$.

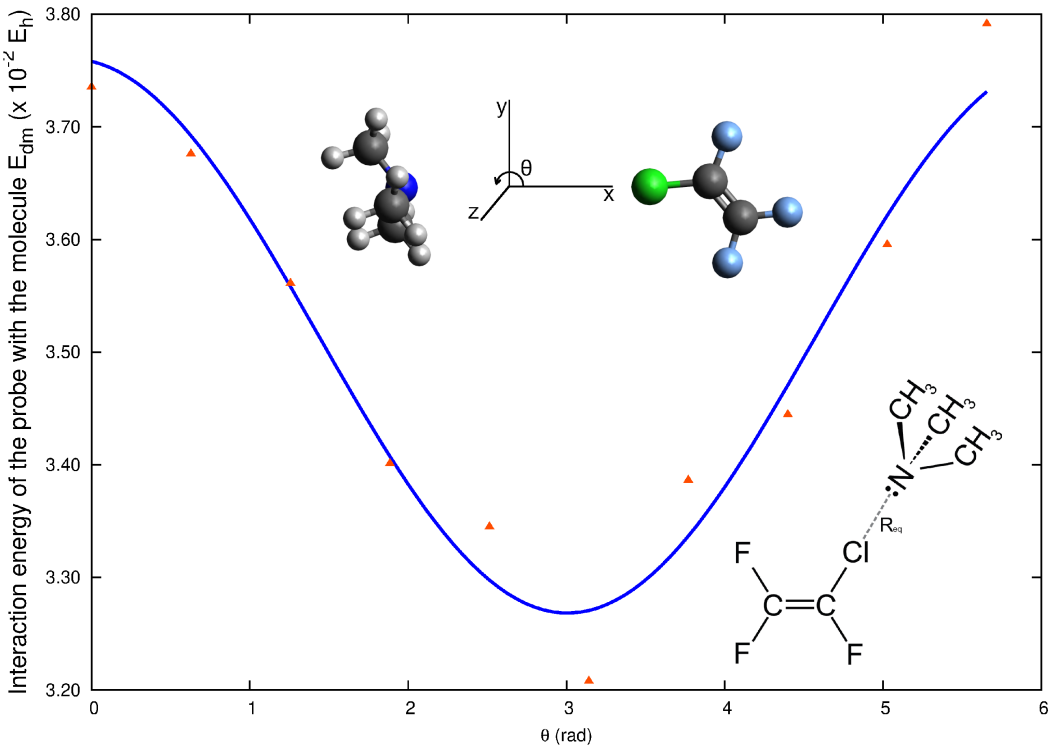

E_{dm} calculation for the $C_2F_3Br\cdots TMA$ system, as shown in the image. Energies are calculated in the midpoint of the interaction. Triangles are the calculated energies of the xy data set, and the line is the sinusoidal fit of equation (5.3).

Source – The authors

Table 11 shows the angles between the electric field and the "bond direction" represented in the systems' Figures. Angles for π-hole bonded $C_2F_3Cl\cdots TMA$ and $C_2F_3Br\cdots TMA$ are larger than that of C_2F_4, but that is expected, because of the symmetry breaking when compared with C_2F_4. For now we think that if we could propose a direction for the intermolecular interaction, the direction of the electric field would be a good candidate. As we've said earlier, this is a matter that deserves more research and consideration in the future.

The electric fields generated by the σ-hole bonded complexes is higher than the ones analysed in π-hole complexes, as expected. The σ-hole bond intensity increases with the increase of the size of the halogen involved in the interaction. We speculate that the chemical properties of the atom are more important than the symmetry breaking effect in determining the bond intensity. Fluorine atoms are the most electronegative, and because of that it tends to remain negative, even at the outside portion of the molecule, therefore

Figure 22 – E_{dm} of σ-bonded $C_2F_3Br \cdots TMA$.

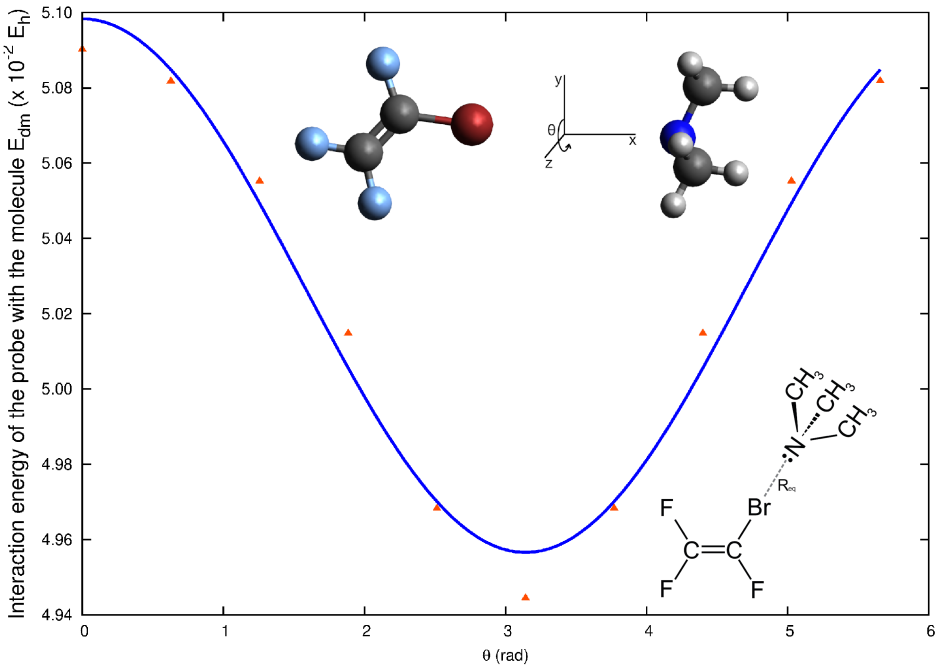

E_{dm} calculation for the $C_2F_3Br \cdots TMA$ system, as shown in the image. Energies are calculated in the midpoint of the interaction. Triangles are the calculated energies of the yz data set, and the line is the sinusoidal fit of equation (5.3).

Source – The authors

Table 11 – Angles between the electric field and the "bond direction".

System	Angle (degrees)
NH_3 dimer	0.7
C_6X_6 - Above the center	0.0
C_2F_4	6.8
C_2F_3Cl - π	18.4
C_2F_3Br - π	22.7
C_2F_3Cl - σ	8.5
C_2F_3Br - σ	8.9

Source – The authors

it cannot produce σ-holes. This effect is smaller the bigger the atom gets, so it is easier for a large halogen, like Br, to generate a σ-hole.

6.2.2 Electric field of the separated parts of the systems

We have also calculated the electric field with the two molecules separated, and compare it with the electric field of the system. We kept the probe in the same position, and removed one of the molecules to perform this calculations. Initially we thought that the interaction would increase the electric field in all cases, because the process induces polarisation, and we believe it would make the electric field increase in the region. However, we have seen that it is not that simple, there could be factors that make the electric field decrease after the bond is established. In our analysed systems, we have one of such cases. We believe that the decrease of the electric field, in this case, has to do with the presence of the four fluorine atoms, which apparently revert part of the original process of creating the hole and thus weaken the electric field.

Every system other than from $C_2F_4 \cdots$ TMA answered as expected, i.e. the sum of the electric field of the parts is smaller than (or equal to) the electric field of the complex (Table 12.

Table 12 – Electric field for separated molecules.

System	A	B	A+B	Complex' EF
$C_2F_4 \cdots$ TMA	0.02	0.06	0.08	0.07
$C_6F_6 \cdots H_2O$ - Above the center	0.04	0.09	0.13	0.14
$C_2F_3Cl \cdots$ TMA - σ	0.01	0.07	0.08	0.08
$C_2F_3Br \cdots$ TMA - σ	0.01	0.08	0.09	0.11
NH_3 dimer	0.10	0.02	0.12	0.12

Source – The authors

Electric fields calculated with only one of the molecules. "A" refers to the first molecule named in the row, and "B" to the second one. "A+B" refers to the sum of their separated electric field, and the Complex' EF is the electric field for the complex, the same shown earlier.

Another interesting fact arises when we analyse the σ-holes of C_2F_3Cl and C_2F_3Br. E_{dm} in this region is almost a perfect fit for the sum of equations (5.3) and (5.4). We can see it in Figure 23, for C_2F_3Br. As we've hinted in section 5.2.2, there seem to be some cases in which we can consider E_{dp} as as interaction between a rigid dipole and a polarisable point, and this is one of those cases. The probe is interacting closely with only one atom in this case, either Cl or Br, and it "notices" its polarisation potential in the neighbourhood. This is similar to what we have seen for chlorobenzene, with the difference that in that case we had a symmetric ring around the probe, and the lone chlorine atom was the standoff.

Figure 23 – E_{dm} of solo C_2F_3Br.

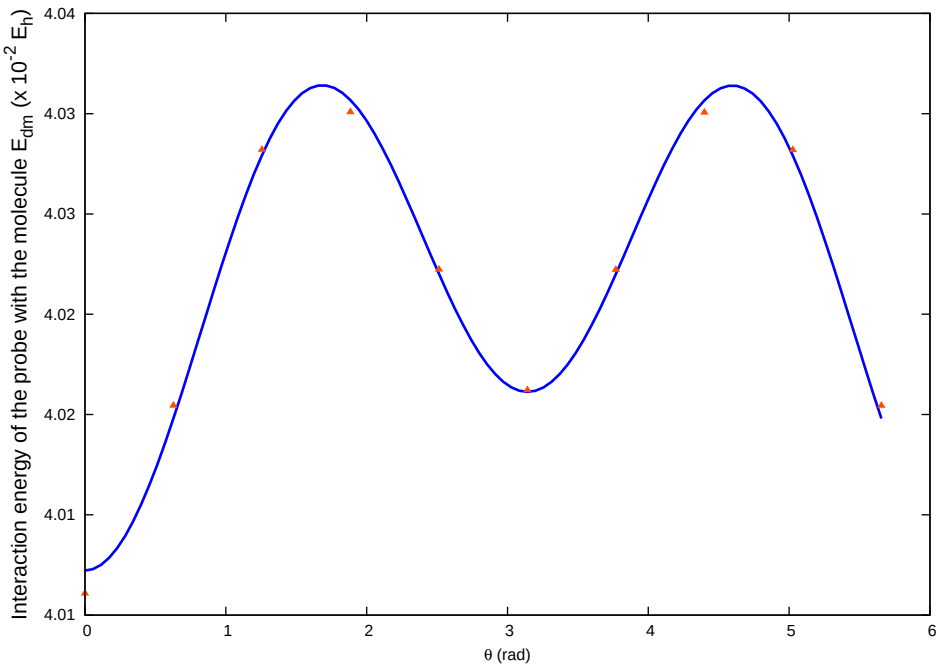

E_{dm} calculation for the C_2F_3Br molecule, as shown in the image. Energies are calculated in the midpoint of the interaction. Triangles are the calculated energies of the yz data set, and the line is the sinusoidal fit of equation (5.3) together with a polarisation energy from equation (5.4).

Source – The authors

The results for the analysis of π- and σ-hole bonds were published in [114].

7 Concluding remarks

This work encompasses the development and applications of a computational isotopic probe to be used as a tool for the study of molecular environments. This is a new method, developed as an alternative to the ones that rely on the MEP, which is an important observable for molecular environments. The isotopic probe is based on the FNMC, which is a correction of the electronic BO Hamiltonian operator. FNMC is what gives us the ability to consider nuclear masses during quantum chemical calculations, and allows us to calculate isotopic dipole moments, a key characteristic of the computational probe.

The probe was developed and tested with simple systems, namely H_2, H_2O, benzene and chlorobenzene, which gave us basic understandings of its interaction with the target molecule. We then started using the probe to study systems of interest in the field, starting with the analysis of the electric field of a phosphine-borane FLP, giving our contribution to the discussion on the mechanism of activation of hydrogen inside the molecule.

Besides, the study of the intermolecular interactions of ten systems already experimentally characterised, has shown that the electric field can be used as a quantifier of molecular bonds, supported by the Hellmann-Feynman theorem. Our results are in accordance with previous qualitative descriptions of molecular interactions, which give us even more security in our method and its results. The probe has proven very reliable in the analysis of the various types of bond, i.e. hydrogen bond, π-hole interactions and σ hole interactions.

Unfortunately, due to its size, the probe cannot be used in every region, but most intermolecular environments are large enough for the probe to "fit". In our view, the use of the isotopic probe as a tool for the analysis of molecular environments has proven successful. And we feel secure in recommending its use in future analysis.

Future work using this method may include:

a) A better understanding of the relationship of E_{dp} with the rotation angle θ, beyond the classical point approximation. A preliminary idea is the utilisation of many classical points to try and fit the $E_{df} + E_{dp}$ curve;

b) Probing of the region between the tip and the substrate in an AFM (atomic force microscope) environment;

c) Study of molecular reactivity, including a better understanding of the effects of lone pairs of electrons on the E_{dm}.

Bibliography

[1] Buckingham, A. D., P. W. Fowler, and Jeremy M. Hutson: *Theoretical studies of van der Waals molecules and intermolecular forces.* Chemical Reviews, 88(6):963–988, 1988. https://doi.org/10.1021/cr00088a008. Cited on page 13.

[2] Maksić, Zvonimir B: *Theoretical Treatment of Large Molecules and Their Interactions: Part 4 Theoretical Models of Chemical Bonding.* Springer, 1991. Cited on page 13.

[3] Gadre, S.R., R.N. Shirsat, and S.R. Garde: *Electrostatics of Atoms and Molecules.* Sangam Books Ltd, 2001, ISBN 8173712964. Cited 4 times in pages 13, 35, 36, and 50.

[4] Politzer, Peter, Jane S. Murray, and Timothy Clark: *Halogen bonding and other σ-hole interactions: a perspective.* Physical Chemistry Chemical Physics, 15(27):11178, 2013. Cited on page 13.

[5] Scrocco, Eolo and Jacopo Tomasi: *Electronic Molecular Structure, Reactivity and Intermolecular Forces: An Euristic Interpretation by Means of Electrostatic Molecular Potentials.* Adv. Quantum Chem., 11:115 – 193, 1978, ISSN 0065-3276. Cited on page 13.

[6] Scrocco, Eolo and Jacopo Tomasi: *The electrostatic molecular potential as a tool for the interpretation of molecular properties.* In *Topics in Current Chemistry Fortschritte der Chemischen Forschung*, pages 95–170. Springer Berlin Heidelberg, 1973. Cited 4 times in pages 13, 14, 35, and 36.

[7] Rico, J. Fernández, R. López, I. Ema, and G. Ramírez: *Electrostatic potentials and fields from density expansions of deformed atoms in molecules.* J. Comput. Chem., 25(11):1347–1354, 2004, ISSN 1096-987X. http://dx.doi.org/10.1002/jcc.20061. Cited 4 times in pages 13, 14, 35, and 36.

[8] Politzer, P, P R Laurence, and K Jayasuriya: *Molecular electrostatic potentials: an effective tool for the elucidation of biochemical phenomena.* Environ. Health Perspect., 61:191–202, sep 1985. Cited 3 times in pages 13, 15, and 35.

[9] Momany, Frank A.: *Determination of partial atomic charges from ab initio molecular electrostatic potentials. Application to formamide, methanol, and formic acid.* The Journal of Physical Chemistry, 82(5):592–601, mar 1978. Cited 2 times in pages 13 and 35.

[10] Cox, S. R. and D. E. Williams: *Representation of the molecular electrostatic potential by a net atomic charge model.* Journal of Computational Chemistry, 2(3):304–323, 1981. Cited 2 times in pages 13 and 35.

[11] Smith, P.H., J.L. Derissen, and F.B. van Duijneveldt: *Intermolecular interactions in crystals of carboxylic acids.* Molecular Physics, 37(2):521–539, feb 1979. Cited 2 times in pages 13 and 35.

[12] Singh, U. Chandra and Peter A. Kollman: *An approach to computing electrostatic charges for molecules.* J. Comput. Chem., 5(2):129–145, apr 1984. Cited 2 times in pages 13 and 35.

[13] Besler, Brent H., Kenneth M. Merz, and Peter A. Kollman: *Atomic charges derived from semiempirical methods.* J. Comput. Chem., 11(4):431–439, may 1990. Cited 2 times in pages 13 and 35.

[14] Rico, J. Fernández, R. López, G. Ramírez, I. Ema, and E. V. Ludeña: *Analytical method for the representation of atoms-in-molecules densities.* J. Comput. Chem., 25(11):1355–1363, may 2004. Cited 3 times in pages 13, 14, and 36.

[15] Rein, Robert: *On Physical Properties and Interactions of Polyatomic Molecules: With Application to Molecular Recognition in Biology.* In *Adv. Quantum Chem.*, pages 335–396. Elsevier, 1973. Cited 2 times in pages 14 and 36.

[16] Stone, A.J. and M. Alderton: *Distributed multipole analysis.* Mol. Phys., 56(5):1047–1064, dec 1985. Cited 2 times in pages 14 and 36.

[17] Yan, Xin Cindy, Michael J. Robertson, Julian Tirado-Rives, and William L. Jorgensen: *Improved Description of Sulfur Charge Anisotropy in OPLS Force Fields: Model Development and Parameterization.* The Journal of Physical Chemistry B, 121(27):6626–6636, jun 2017. Cited on page 14.

[18] Kramer, Christian, Alexander Spinn, and Klaus R. Liedl: *Charge Anisotropy: Where Atomic Multipoles Matter Most.* J. Chem. Theory Comput., 10(10):4488–4496, oct 2014. Cited on page 14.

[19] Bonaccorsi, Rosanna, Eolo Scrocco, and Jacopo Tomasi: *Group contributions to the electrostatic molecular potential.* J. Am. Chem. Soc., 98(14):4049–4054, jul 1976. Cited 2 times in pages 14 and 36.

[20] Bonaccorsi, Rosanna, Eolo Scrocco, and Jacopo Tomasi: *An approximate expression of the electrostatic molecular potential in terms of completely transferable group contributions.* J. Am. Chem. Soc., 99(14):4546–4554, jun 1977. Cited 2 times in pages 14 and 36.

[21] Julg, André: *On the description of molecules using point charges and electric moments*. In *Topics in Current Chemistry*, pages 1–37. Springer-Verlag, 1975. Cited 2 times in pages 14 and 36.

[22] Stewart, Robert F.: *V. One-Electron Density Functions and Many-Centered Finite Multipole Expansions*. Isr. J. Chem., 16(2-3):124–131, 1977. Cited 2 times in pages 14 and 36.

[23] Bentley, John: *Collision-induced atomic dipole moments*. The Journal of Chemical Physics, 70(6):3125–3129, mar 1979. Cited 2 times in pages 14 and 36.

[24] Amos, A.T. and R.J. Crispin: *Intermolecular forces between large molecules*. Mol. Phys., 31(1):159–176, jan 1976. Cited 2 times in pages 14 and 36.

[25] Stone, A.J.: *Distributed multipole analysis, or how to describe a molecular charge distribution*. Chem. Phys. Lett., 83(2):233–239, oct 1981. Cited 2 times in pages 14 and 36.

[26] Rico, J. Fernández, R. López, and G. Ramírez: *Analysis of the molecular density*. The Journal of Chemical Physics, 110(9):4213–4220, mar 1999. Cited 2 times in pages 14 and 36.

[27] Rico, J. Fernández, R. López, I. Ema, and G. Ramírez: *Analysis of the molecular density: STO densities*. The Journal of Chemical Physics, 117(2):533–540, jul 2002. Cited 2 times in pages 14 and 36.

[28] Botu, V., R. Batra, J. Chapman, and R. Ramprasad: *Machine Learning Force Fields: Construction, Validation, and Outlook*. The Journal of Physical Chemistry C, 121(1):511–522, dec 2016. Cited 2 times in pages 14 and 15.

[29] Ren, Pengyu and Jay W Ponder: *Consistent treatment of inter-and intramolecular polarization in molecular mechanics calculations*. Journal of computational chemistry, 23(16):1497–1506, 2002. Cited on page 14.

[30] Bertoni, Colleen, Lyudmila V Slipchenko, Alston J Misquitta, and Mark S Gordon: *Multipole moments in the effective fragment potential method*. The Journal of Physical Chemistry A, 121(9):2056–2067, 2017. Cited on page 14.

[31] Bader, Richard F. W., Marshall T. Carroll, James R. Cheeseman, and Cheng Chang: *Properties of atoms in molecules: atomic volumes*. Journal of the American Chemical Society, 109(26):7968–7979, dec 1987. Cited 3 times in pages 14, 36, and 51.

[32] Wang, Hui, Weizhou Wang, and Wei Jun Jin: *σ-Hole Bond vs π-Hole Bond: A Comparison Based on Halogen Bond*. Chemical Reviews, 116(9):5072–5104, feb 2016. Cited 5 times in pages 14, 16, 37, 54, and 55.

[33] Politzer, Peter, Jane S. Murray, and Timothy Clark: *Halogen bonding: an electrostatically-driven highly directional noncovalent interaction.* Physical Chemistry Chemical Physics, 12(28):7748, 2010. Cited 4 times in pages 14, 35, 51, and 52.

[34] Hunter, Christopher A.: *Quantifying Intermolecular Interactions: Guidelines for the Molecular Recognition Toolbox.* Angewandte Chemie International Edition, 43(40):5310–5324, oct 2004. Cited 4 times in pages 14, 35, 37, and 51.

[35] Politzer, Peter and Jane S. Murray: *The Hellmann-Feynman theorem: a perspective.* Journal of Molecular Modeling, 24(9), aug 2018. Cited 3 times in pages 14, 35, and 51.

[36] Politzer, Peter, Linda N. Domelsmith, Per Sjöberg, and Jack Alster: *Electrostatic potentials of strained systems: nitrocyclopropane.* Chem. Phys. Lett., 92(4):366–370, oct 1982. Cited 2 times in pages 15 and 35.

[37] Culver, Heidi R., John R. Clegg, and Nicholas A. Peppas: *Analyte-Responsive Hydrogels: Intelligent Materials for Biosensing and Drug Delivery.* Accounts of Chemical Research, 50(2):170–178, feb 2017. Cited on page 15.

[38] O'Meara, Matthew J., Andrew Leaver-Fay, Michael D. Tyka, Amelie Stein, Kevin Houlihan, Frank DiMaio, Philip Bradley, Tanja Kortemme, David Baker, Jack Snoeyink, and Brian Kuhlman: *Combined Covalent-Electrostatic Model of Hydrogen Bonding Improves Structure Prediction with Rosetta.* Journal of Chemical Theory and Computation, 11(2):609–622, jan 2015. Cited on page 15.

[39] Kocman, Mikuláš, Martin Pykal, and Petr Jurečka: *Electric quadrupole moment of graphene and its effect on intermolecular interactions.* Physical Chemistry Chemical Physics, 16(7):3144, 2014. Cited on page 15.

[40] Wang, Bo and Donald G. Truhlar: *Screened Electrostatic Interactions in Molecular Mechanics.* Journal of Chemical Theory and Computation, 10(10):4480–4487, sep 2014. Cited on page 15.

[41] Mohallem, J R: *Effective three-body Born-Oppenheimer Hamiltonian including adiabatic corrections.* Journal of Physics B: Atomic, Molecular and Optical Physics, 32(15):3805–3811, aug 1999. Cited 2 times in pages 15 and 32.

[42] MOHALLEM, J. R., FLÁVIA ROLIM, and CRISTINA P. GONÇALVES: *The modified electronic mass approach for the adiabatic corrections in H2.* Molecular Physics, 99(2):87–90, 2001. `https://doi.org/10.1080/00268970109483855`. Cited 2 times in pages 15 and 32.

[43] Mohallem, José R.: *Evidences of molecular structure beyond the BornOppenheimer approximation: the model hamiltonian*. Journal of Molecular Structure: {THEOCHEM}, 709(13):11 – 13, 2004, ISSN 0166-1280. A Collection of Papers Presented at the 29th International Congress of Theoretical Chemists of Latin Expression, Marrakech, Morocco, 8-12 September, 2003. Cited 2 times in pages 15 and 22.

[44] Gonçalves, Cristina P., Flávia Rolim, Vinícius C. Mota, and José R. Mohallem: *Molecular dynamics simulations of isotope compounds of hydrogen atoms: prospects and progress*. Journal of Molecular Structure: THEOCHEM, 580(1):33 – 38, 2002, ISSN 0166-1280. `http://www.sciencedirect.com/science/article/pii/S0166128001005929`. Cited 2 times in pages 15 and 32.

[45] Gonçalves, Cristina P and José R Mohallem: *Point group symmetries of the molecular orbitals of HD+ beyond the BornOppenheimer approximation*. Chemical Physics Letters, 367(5):533 – 536, 2003, ISSN 0009-2614. `http://www.sciencedirect.com/science/article/pii/S0009261402017347`. Cited 2 times in pages 15 and 32.

[46] Assafrão, Denise and José R Mohallem: *The isotopic dipole moment of HDO*. Journal of Physics B: Atomic, Molecular and Optical Physics, 40(5):F85–F91, feb 2007. Cited 2 times in pages 15 and 32.

[47] Diniz, Leonardo G. and José R. Mohallem: *Towards universal potentials for (H2)2 and isotopic variants: Post-BornOppenheimer contributions*. The Journal of Chemical Physics, 128(21):214306, 2008. `https://doi.org/10.1063/1.2929832`. Cited 3 times in pages 15, 32, and 33.

[48] Arapiraca, Antônio Francisco Cruz: *Efeitos isotópicos em espectroscopia rotacional molecular com vistas a aplicações em radioastronomia*. Doutorado em física, Universidade Federal de Minas Gerais, 2012. Cited 3 times in pages 15, 22, and 34.

[49] Arapiraca, A. F. C., Dan Jonsson, and J. R. Mohallem: *Vibrationally averaged post Born-Oppenheimer isotopic dipole moment calculations approaching spectroscopic accuracy*. The Journal of Chemical Physics, 135(24), 2011. Cited 4 times in pages 15, 22, 34, and 38.

[50] Arapiraca, A.F.C. and J.R. Mohallem: *{DFT} vibrationally averaged isotopic dipole moments of propane, propyne and water isotopologues*. Chem. Phys. Lett., 609:123 – 128, 2014, ISSN 0009-2614. Cited 3 times in pages 15, 32, and 34.

[51] Gonçalves, Cristina P. and José R. Mohallem: *A new algorithm to handle finite nuclear mass effects in electronic calculations: The ISOTOPE program*. J. Comput. Chem., 25(14):1736–1739, 2004, ISSN 1096-987X. `http://dx.doi.org/10.1002/jcc.20093`. Cited 2 times in pages 15 and 22.

[52] Aidas, Kestutis *et al.*: *The Dalton quantum chemistry program system.* Wiley Interdisciplinary Reviews: Computational Molecular Science, 4(3):269–284, sep 2013. Cited 2 times in pages 15 and 42.

[53] *Dalton, a molecular electronic structure program, Release v2016.2 (2019).* `http://daltonprogram.org`. Cited 2 times in pages 15 and 42.

[54] Mark Gordon's Quantum Theory Group: *GAMESS.* `http://www.msg.ameslab.gov/index.html`. Cited 2 times in pages 15 and 42.

[55] Hellmann, Hans: *Einführung in die Quantenchemie.* F. Deuticke, 1937. Cited on page 15.

[56] Feynman, R. P.: *Forces in Molecules.* Phys. Rev., 56(4):340–343, aug 1939. Cited 2 times in pages 15 and 51.

[57] Steed, Jonathan W. and Jerry L. Atwood: *Supramolecular Chemistry.* Wiley, 2013, ISBN 978-0-470-51233-3. Cited on page 15.

[58] Coutinho, Kaline: *Metodos de Quimica Teorica e Modelagem Molecular.* Livraria da Física, 2007, ISBN 9788588325876. Cited 5 times in pages 17, 20, 22, 24, and 28.

[59] Pack, Russell T and Joseph O. Hirschfelder: *Separation of Rotational Coordinates from the NElectron Diatomic Schrödinger Equation.* The Journal of Chemical Physics, 49(9):4009–4020, 1968. `https://doi.org/10.1063/1.1670711`. Cited on page 18.

[60] Linstrom, P.J. and W.G. Mallard: *Phase Transition Enthalpy Measurements of Organic and Organometallic Compounds.* National Institute of Standards and Technology, Gaithersburg MD, 2020. Cited on page 23.

[61] Hohenberg, P. and W. Kohn: *Inhomogeneous Electron Gas.* Phys. Rev., 136:B864–B871, Nov 1964. `https://link.aps.org/doi/10.1103/PhysRev.136.B864`. Cited on page 28.

[62] Kohn, W. and L. J. Sham: *Self-Consistent Equations Including Exchange and Correlation Effects.* Physical Review, 140(4A):A1133–A1138, nov 1965. Cited on page 29.

[63] Brading, Katherine, Castellani Elena and Nicholas Teh: *Symmetry and Symmetry Breaking.* In Zalta, Edward N. (editor): *The Stanford Encyclopedia of Philosophy.* Metaphysics Research Lab, Stanford University, winter 2017 edition, 2017. Cited on page 32.

[64] Gonçalves, Cristina P. and José R. Mohallem: *MO theory of isotope symmetry breaking in HDO and HD.* Chemical Physics Letters, 380(3):378 – 382, 2003, ISSN 0009-2614. http://www.sciencedirect.com/science/article/pii/S0009261403016233. Cited on page 32.

[65] Mohallem, José R. and Leonardo G. Diniz: *Isotopic dipole moments in water clusters.* International Journal of Quantum Chemistry, 111(78):1493–1497, 2011. https://onlinelibrary.wiley.com/doi/abs/10.1002/qua.22686. Cited on page 32.

[66] Eduardo Fleuri Mortimer, Andréa Horta Machado: *Química.* Scipione, São Paulo, 2nd edition, 2013. Cited on page 34.

[67] Arapiraca, A. F. C. and J. R. Mohallem: *Vibrationally averaged dipole moments of methane and benzene isotopologues.* The Journal of Chemical Physics, 144(14), 2016. Cited on page 34.

[68] Weiner, P. K., R. Langridge, J. M. Blaney, R. Schaefer, and P. A. Kollman: *Electrostatic potential molecular surfaces.* Proceedings of the National Academy of Sciences, 79(12):3754–3758, jun 1982. Cited 2 times in pages 37 and 51.

[69] Parker, Anna J., John Stewart, Kelling J. Donald, and Carol A. Parish: *Halogen Bonding in DNA Base Pairs.* Journal of the American Chemical Society, 134(11):5165–5172, mar 2012. Cited on page 37.

[70] Williams, Thomas, Colin Kelley, and many others: *Gnuplot 4.6: an interactive plotting program.* http://gnuplot.sourceforge.net/, April 2013. Cited on page 42.

[71] Keutsch, F. N. and R. J. Saykally: *Water clusters: Untangling the mysteries of the liquid, one molecule at a time.* Proceedings of the National Academy of Sciences, 98(19):10533–10540, sep 2001. Cited on page 44.

[72] Bansmer, Stephan E., Arne Baumert, Stephan Sattler, Inken Knop, Delphine Leroy, Alfons Schwarzenboeck, Tina Jurkat-Witschas, Christiane Voigt, Hugo Pervier, and Biagio Esposito: *Design, Construction and Commissioning of the Braunschweig Icing Wind Tunnel.* Atmospheric Measurement Techniques Discussions, pages 1–51, nov 2017. Cited on page 44.

[73] Debenedetti, Pablo G. and H. Eugene Stanley: *Supercooled and Glassy Water.* Physics Today, 56(6):40–46, jun 2003. Cited on page 44.

[74] Fillaux, François: *The quantum phase-transitions of water.* EPL (Europhysics Letters), 119(4):40008, aug 2017. Cited on page 44.

[75] Stanley, H. Eugene and Osamu Mishima: *The relationship between liquid, supercooled and glassy water*. Nature, 396(6709):329–335, nov 1998. Cited on page 44.

[76] Mahadevi, A. Subha and G. Narahari Sastry: *Cooperativity in Noncovalent Interactions*. Chemical Reviews, 116(5):2775–2825, feb 2016. Cited 2 times in pages 44 and 52.

[77] Arunan, Elangannan, Gautam R. Desiraju, Roger A. Klein, Joanna Sadlej, Steve Scheiner, Ibon Alkorta, David C. Clary, Robert H. Crabtree, Joseph J. Dannenberg, Pavel Hobza, Henrik G. Kjaergaard, Anthony C. Legon, Benedetta Mennucci, and David J. Nesbitt: *Defining the hydrogen bond: An account (IUPAC Technical Report)*. Pure and Applied Chemistry, 83(8), jan 2011. Cited on page 44.

[78] Huang, Yongli, Xi Zhang, Zengsheng Ma, Yichun Zhou, Weitao Zheng, Ji Zhou, and Chang Q. Sun: *Hydrogen-bond relaxation dynamics: Resolving mysteries of water ice*. Coordination Chemistry Reviews, 285:109–165, feb 2015. Cited on page 44.

[79] Mohallem, José R., Paulo F. G. Velloso, and Antonio F. C. Arapiraca: *Probing molecular environments with a fictitious isotopic dipole*. International Journal of Quantum Chemistry, page e25917, feb 2019. Cited 3 times in pages 48, 51, and 85.

[80] Lewis, Gilbert Newton: *Valence and the Structure of Atoms and Molecules*. Dover Publications Inc., 1923, ISBN 0486615553. Cited on page 48.

[81] `http://bit.ly/2y5XQXc`. Cited on page 48.

[82] Stephan, Douglas W.: *"Frustrated Lewis pairs": a concept for new reactivity and catalysis*. Organic & Biomolecular Chemistry, 6(9):1535, 2008. Cited on page 49.

[83] Stephan, Douglas W. and Gerhard Erker: *Frustrated Lewis Pairs: Metal-free Hydrogen Activation and More*. Angew. Chem. Int. Ed., 49(1):46–76, dec 2009. Cited on page 49.

[84] `http://bit.ly/2Gquk2O`. Cited on page 49.

[85] Rokob, Tibor András, Andrea Hamza, and Imre Pápai: *Rationalizing the Reactivity of Frustrated Lewis Pairs: Thermodynamics of H2Activation and the Role of Acid-Base Properties*. J. Am. Chem. Soc., 131(30):10701–10710, aug 2009. Cited on page 49.

[86] Welch, G. C., R. R. S. Juan, J. D. Masuda, and D. W. Stephan: *Reversible, Metal-Free Hydrogen Activation*. Science, 314(5802):1124–1126, nov 2006. Cited on page 49.

[87] Welch, Gregory C. and Douglas W. Stephan: *Facile Heterolytic Cleavage of Dihydrogen by Phosphines and Boranes.* J. Am. Chem. Soc., 129(7):1880–1881, feb 2007. Cited on page 49.

[88] Grimme, Stefan, Holger Kruse, Lars Goerigk, and Gerhard Erker: *The Mechanism of Dihydrogen Activation by Frustrated Lewis Pairs Revisited.* Angew. Chem. Int. Ed., 49(8):1402–1405, jan 2010. Cited on page 49.

[89] Schirmer, Birgitta and Stefan Grimme: *Electric field induced activation of H2—Can DFT do the job?* Chem. Commun., 46(42):7942, 2010. Cited on page 49.

[90] Rokob, Tibor András, Imre Bakó, András Stirling, Andrea Hamza, and Imre Pápai: *Reactivity Models of Hydrogen Activation by Frustrated Lewis Pairs: Synergistic Electron Transfers or Polarization by Electric Field?* J. Am. Chem. Soc., 135(11):4425–4437, mar 2013. Cited 3 times in pages 49, 50, and 78.

[91] Stephan, Douglas W.: *Frustrated Lewis Pairs.* Journal of the American Chemical Society, 137(32):10018–10032, aug 2015. Cited on page 49.

[92] Arndt, Sebastian, Matthias Rudolph, and A. Stephen K. Hashmi: *Gold-based frustrated Lewis acid/base pairs (FLPs).* Gold Bulletin, 50(3):267–282, sep 2017. Cited on page 49.

[93] Liu, Lei, Binit Lukose, and Bernd Ensing: *Hydrogen Activation by Frustrated Lewis Pairs Revisited by Metadynamics Simulations.* The Journal of Physical Chemistry C, 121(4):2046–2051, jan 2017. Cited 4 times in pages 49, 50, 51, and 79.

[94] Liu, Lei, Jan Gerit Brandenburg, and Stefan Grimme: *On the hydrogen activation by frustrated Lewis pairs in the solid state: benchmark studies and theoretical insights.* Philosophical Transactions of the Royal Society A: Mathematical, Physical and Engineering Sciences, 375(2101):20170006, jul 2017. Cited 2 times in pages 49 and 50.

[95] Özgün, Thomas, Ke Yin Ye, Constantin G. Daniliuc, Birgit Wibbeling, Lei Liu, Stefan Grimme, Gerald Kehr, and Gerhard Erker: *Why Does the Intramolecular Trimethylene-Bridged Frustrated Lewis Pair Mes2 PCH2 CH2 CH2 B(C6 F5)2 Not Activate Dihydrogen?* Chemistry - A European Journal, 22(17):5988–5995, mar 2016. Cited on page 49.

[96] Rokob, Tibor András, Andrea Hamza, András Stirling, Tibor Soós, and Imre Pápai: *Turning Frustration into Bond Activation: A Theoretical Mechanistic Study on Heterolytic Hydrogen Splitting by Frustrated Lewis Pairs.* Angewandte Chemie International Edition, 47(13):2435–2438, mar 2008. Cited on page 50.

[97] Soliva, Robert, Francisco J. Luque, and Modesto Orozco: *Reliability of MEP and MEP-derived properties computed from DFT methods for molecules containing P, S and CL.* Theoretical Chemistry Accounts: Theory, Computation, and Modeling (Theoretica Chimica Acta), 98(1):42–49, oct 1997. Cited on page 50.

[98] Soliva, Robert, Modesto Orozco, and F. Javier Luque: *Suitability of density functional methods for calculation of electrostatic properties.* J. Comput. Chem., 18(8):980–991, jun 1997. Cited on page 50.

[99] Hellmann, H.: *Zur Rolle der kinetischen Elektronenenergie für die zwischenatomaren Kräfte.* Zeitschrift für Physik, 85(3-4):180–190, mar 1933. Cited on page 51.

[100] Lu, Yunxiang, Jianwei Zou, Hongqing Wang, Qingsen Yu, Huaxin Zhang, and Yongjun Jiang: *Triangular Halogen Trimers. A DFT Study of the Structure, Cooperativity, and Vibrational Properties.* The Journal of Physical Chemistry A, 109(51):11956–11961, dec 2005. Cited on page 52.

[101] Voth, A. R., F. A. Hays, and P. S. Ho: *Directing macromolecular conformation through halogen bonds.* Proceedings of the National Academy of Sciences, 104(15):6188–6193, mar 2007. Cited on page 52.

[102] Alkorta, Ibon, Isabel Rozas, and Jose Elguero: *An Attractive Interaction between the π-Cloud of C6F6 and Electron-Donor Atoms.* The Journal of Organic Chemistry, 62(14):4687–4691, jul 1997. Cited on page 52.

[103] Alkorta, Ibon, Isabel Rozas, María Luisa Jimeno, and José Elguero: *A Theoretical and Experimental Study of the Interaction of C6F6 with Electron Donors.* Structural Chemistry, 12(6):459–464, 2001. Cited on page 52.

[104] *Water.* `https://www.un.org/en/sections/issues-depth/water/`. Cited on page 52.

[105] *World Water Day 2018: Nature for Water.* `https://whc.unesco.org/en/news/1798`. Cited on page 52.

[106] Mooibroek, Tiddo J., Patrick Gamez, and Jan Reedijk: *Lone pair–π interactions: a new supramolecular bond?* CrystEngComm, 10(11):1501, 2008. Cited on page 52.

[107] Ma, Ning, Yu Zhang, Baoming Ji, Anmin Tian, and Weizhou Wang: *Structural Competition between Halogen Bonds and Lone-Pair$\cdots\pi$ Interactions in Solution.* ChemPhysChem, 13(6):1411–1414, feb 2012. Cited on page 52.

[108] Korenaga, Toshinobu, Taeko Shoji, Kazutaka Onoue, and Takashi Sakai: *Demonstration of the existence of intermolecular lone pair$\cdots\pi$ interaction between alcoho-*

lic oxygen and the C6F5 group in organic solvent. Chemical Communications, (31):4678, 2009. Cited on page 52.

[109] Amicangelo, Jay C., Daniel G. Irwin, Cynthia J. Lee, Natalie C. Romano, and Nancy L. Saxton: *Experimental and Theoretical Characterization of a Lone Pair-π Complex: Water–Hexafluorobenzene.* The Journal of Physical Chemistry A, 117(6):1336–1350, nov 2012. Cited 5 times in pages 52, 53, 55, 80, and 81.

[110] Egli, Martin and Sanjay Sarkhel: *Lone Pair-Aromatic Interactions: To Stabilize or Not to Stabilize.* Accounts of Chemical Research, 40(3):197–205, mar 2007. Cited on page 52.

[111] Grimme, Stefan, Jens Antony, Stephan Ehrlich, and Helge Krieg: *A consistent and accurate ab initio parametrization of density functional dispersion correction (DFT-D) for the 94 elements H-Pu.* The Journal of Chemical Physics, 132(15):154104, apr 2010. Cited on page 52.

[112] Jurečka, Petr, Jiří Šponer, Jiří Černý, and Pavel Hobza: *Benchmark database of accurate (MP2 and CCSD(T) complete basis set limit) interaction energies of small model complexes, DNA base pairs, and amino acid pairs.* Phys. Chem. Chem. Phys., 8(17):1985–1993, 2006. Cited 2 times in pages 53 and 80.

[113] Geboes, Yannick, Frank De Proft, and Wouter A. Herrebout: *Expanding Lone Pair$\cdots\pi$ Interactions to Nonaromatic Systems and Nitrogen Bases: Complexes of C2F3X (X = F, Cl, Br, I) and TMA-d 9.* The Journal of Physical Chemistry A, 119(22):5597–5606, may 2015. Cited 4 times in pages 56, 82, 83, and 84.

[114] Velloso, Paulo F. G. and José R. Mohallem: *Probing internal electric fields of - and -hole bonds.* International Journal of Quantum Chemistry, n/a(n/a):e26116. `https://onlinelibrary.wiley.com/doi/abs/10.1002/qua.26116`. Cited 2 times in pages 63 and 85.

Appendix

APPENDIX A – Molecular Cartesian coordinates

In this appendix, we show the Cartesian coordinates for all the systems described in this work. All coordinates are in Angstroms.

Table 13 – Cartesian coordinates for the phosphine-borane FLP.

Atom	x	y	z	Atom	x	y	z
C	4.367882	-0.047101	-1.420151	C	2.706810	-0.673442	2.251067
C	3.653265	0.953404	-0.782326	C	-2.763434	0.237760	3.046858
C	2.275799	0.976986	-0.895767	C	-1.525137	-1.164313	4.674664
C	1.553258	0.009827	-1.591124	C	0.171547	1.818542	3.151437
C	2.316222	-0.965444	-2.233002	C	1.602672	2.357901	2.973412
C	3.696901	-1.006912	-2.163243	C	-0.223271	2.034563	4.619726
B	-0.015855	-0.019597	-1.582477	C	-0.710412	2.702797	2.245136
C	-0.826679	1.324064	-1.582283	C	1.256479	-2.483355	3.039272
C	-2.006233	1.472533	-0.856085	C	1.896071	-0.693333	4.631720
C	-2.672126	2.678012	-0.736549	H	-3.681113	-0.304958	3.299060
C	-2.181421	3.791034	-1.399007	H	-2.511524	-1.540919	4.969754
C	-1.035188	3.683009	-2.172436	H	-2.858326	-2.393617	2.674464
C	-0.382049	2.466213	-2.247837	H	-2.707464	1.095817	3.715582
F	-3.762163	2.778072	0.016026	H	-2.872537	0.596737	2.024488
F	-2.534879	0.437984	-0.202231	H	-1.278684	-0.336166	5.340007
F	-2.808475	4.950721	-1.302427	H	-1.275018	1.825215	4.810976
F	-0.576659	4.743814	-2.825290	H	-0.810440	-1.966205	4.855429
F	0.714206	2.417607	-3.005353	H	-2.077225	-1.630524	1.282677
F	1.647997	1.970722	-0.266871	H	-1.765641	2.435847	2.268834
F	1.721898	-1.911210	-2.961176	H	-1.163868	-2.724208	2.328131
F	4.289324	1.867989	-0.058807	H	-0.051955	3.084565	4.884346
F	4.382650	-1.952996	-2.792876	H	0.371715	1.424460	5.300155
F	5.686182	-0.082053	-1.329237	H	-0.628833	3.745792	2.571662
C	-0.774828	-1.392995	-1.550591	H	0.503522	-2.857023	3.732115
C	-2.002164	-1.583697	-2.184847	H	-0.366849	2.648003	1.209523
C	-2.728488	-2.756088	-2.080832	H	1.074240	-0.887073	5.321936
C	-2.231464	-3.795905	-1.309224	H	0.973077	-2.767729	2.026980
C	-1.006468	-3.659565	-0.677234	H	2.191762	-3.004271	3.272014
C	-0.297316	-2.482295	-0.825300	H	2.237805	0.328415	4.792576
F	-2.920829	-4.917034	-1.185361	H	2.723347	-1.356311	4.910958
F	-3.891977	-2.894148	-2.704540	H	1.593006	3.430834	3.194745
F	-0.531121	-4.647069	0.073371	H	2.321061	1.899846	3.652095
F	-2.525448	-0.616449	-2.938986	H	1.962978	2.243379	1.952197
F	0.878636	-2.417517	-0.200638	H	2.481777	-0.973482	1.224933
C	-1.924208	-1.945061	2.317658	H	3.002681	0.374323	2.243087
C	-1.575923	-0.729827	3.202566	H	3.571384	-1.255608	2.589735
P	0.025749	0.030687	2.460922				
C	1.504913	-0.969538	3.172601				

Source – Reference [90]

Table 14 – Cartesian coordinates for the TS1 of phosphine-borane FLP.

Atom	x	y	z	Atom	x	y	z
H	-3.409338	3.418224	-3.097296	C	1.864947	1.377899	-0.154472
H	-5.215611	1.634499	-3.140616	H	-1.545434	3.535702	1.327550
H	-2.930975	1.287943	-3.829260	C	2.746789	3.638135	0.394544
F	1.102698	3.747691	-2.873672	H	-5.726552	-0.392232	0.191474
C	-3.323029	3.209034	-2.011053	H	-0.821024	0.061322	-0.801093
H	-4.053291	3.845607	-1.479513	H	-0.154479	-0.415527	-0.796524
H	-2.301877	3.513402	-1.706071	F	-0.067417	-2.616894	-0.894412
F	3.993099	-4.988845	-1.314496	C	2.550866	2.280244	0.694921
C	-5.009973	1.306289	-2.099475	B	1.461462	-0.080845	0.359438
H	-5.746813	1.772618	-1.418759	F	3.389887	4.419403	1.281085
F	5.415202	-2.768239	-0.417579	C	-3.350090	-1.499825	-0.698841
C	-2.603308	1.011850	-2.801299	H	-2.312926	-1.538143	-1.083286
H	-5.158197	3.435195	0.047882	C	-4.981452	-0.624074	0.976870
C	-3.548934	1.697310	-1.772737	C	-3.523282	-0.485113	0.472819
F	0.839634	1.165002	-2.311659	H	-3.592053	-2.516412	-0.314819
H	-5.118085	0.206856	-2.067618	H	-5.180058	0.025267	1.847960
C	1.614104	3.303512	-1.703155	C	-3.356517	2.027447	2.700880
H	-1.558416	1.365828	-2.680381	H	-5.122937	-1.679318	1.296622
F	2.457109	5.511331	-1.093604	F	2.989095	1.866315	1.932971
C	3.354716	-3.834847	-1.030856	H	-3.566222	2.860475	3.408226
C	4.079375	-2.721978	-0.565177	H	-4.030372	1.192153	2.965748
H	-2.677618	4.288453	0.164899	H	-2.310396	1.718765	2.899208
H	-2.590705	-0.091937	-2.755796	C	0.937087	-0.178338	1.853941
C	1.454015	1.935858	-1.383934	F	0.027726	2.060419	1.857714
H	-5.206526	3.826903	1.789108	F	1.641171	-2.476949	2.186757
C	2.275998	4.190969	-0.815759	H	-1.535499	-1.078935	1.197902
F	1.324031	-4.937630	-1.520459	C	-2.572406	-1.013421	1.582769
C	-5.001266	3.010959	1.058540	H	-2.568827	-0.391462	2.492847
C	1.948976	-3.790308	-1.135355	C	0.432883	0.965007	2.546999
F	4.064769	-0.502495	0.252593	C	1.233354	-1.288184	2.690515
C	3.365502	-1.553504	-0.249646	H	-2.885751	-2.045482	1.861593
H	-5.740277	2.204354	1.225396	C	0.319757	1.044989	3.940880
C	-2.606607	3.795952	1.149917	C	1.146026	-1.239066	4.090096
H	-2.924402	4.540762	1.911661	F	-0.147152	2.146953	4.548639
H	-4.022602	-1.301833	-1.554141	F	1.515313	-2.271590	4.861299
C	1.279504	-2.597396	-0.790125	C	0.714038	-0.059164	4.709457
C	1.965690	-1.434394	-0.337179	F	0.674495	0.026378	6.042723
P	-2.857185	1.277696	-0.018785				
C	-3.538403	2.549458	1.253427				

Source – Reference [93]

Table 15 – Cartesian coordinates for the ammonia dimer.

Atom	x	y	z
N	-1.578718	-0.046611	0.000000
N	1.578718	0.046611	0.000000
H	-2.158621	0.136396	-0.809565
H	-2.158621	0.136396	0.809565
H	-0.849471	0.658193	0.000000
H	2.158621	-0.136396	-0.809565
H	0.849471	-0.658193	0.000000
H	2.158621	-0.136396	0.809565

Source – Reference [112]

Table 16 – Cartesian coordinates for $C_6F_6 \cdots H_2O$ - Above the center.

Atom	x	y	z
C	0.00000000	1.39304900	-0.34466900
C	1.20724000	0.69672900	-0.34493200
C	-1.20724000	0.69672900	-0.34493200
C	1.20724000	-0.69672900	-0.34493200
C	-1.20724000	-0.69672900	-0.34493200
C	0.00000000	-1.39304900	-0.34466900
F	0.00000000	2.73436200	-0.33612000
F	2.36792500	1.36760700	-0.33723100
F	-2.36792500	1.36760700	-0.33723100
F	2.36792500	-1.36760700	-0.33723100
F	-2.36792500	-1.36760700	-0.33723100
F	0.00000000	-2.73436200	-0.33612000
O	0.00000000	0.00000000	2.94256400
H	0.00000000	0.76397200	3.53216800
H	0.00000000	-0.76397200	3.53216800

Source – Reference [109]

Table 17 – Cartesian coordinates for $C_6F_6 \cdots H_2O$ - Above the bond.

Atom	x	y	z
C	0.24673000	0.29276100	1.39331600
C	0.59166000	-0.86383400	0.69667800
C	-0.09867500	1.45078900	0.69705700
C	0.59166000	-0.86383400	-0.69667800
C	-0.09867500	1.45078900	-0.69705700
C	0.24673000	0.29276100	-1.39331600
F	0.24162200	0.29126700	2.73423200
F	0.91408200	-1.97733000	1.36808900
F	-0.42839400	2.56347900	1.36807600
F	0.91408200	-1.97733000	-1.36808900
F	-0.42839400	2.56347900	-1.36807600
F	0.24162200	0.29126700	-2.73423200
O	-2.16785400	-2.52069500	0.00000000
H	-2.31266900	-3.09224600	0.76398200
H	-2.31266900	-3.09224600	-0.76398200

Source – Reference [109]

Table 18 – Cartesian coordinates for $C_6F_6 \cdots H_2O$ - Above the atom.

Atom	x	y	z
C	-0.61651300	-1.02744100	0.00000000
C	-0.42290900	-0.35993400	1.20733200
C	-0.42290900	-0.35993400	-1.20733200
C	-0.03475200	0.97919500	1.20772100
C	-0.03475200	0.97919500	-1.20772100
C	0.15938100	1.64893600	0.00000000
F	-0.98124000	-2.31834500	0.00000000
F	-0.60280700	-1.00600500	2.36706900
F	-0.60280700	-1.00600500	-2.36706900
F	0.15208200	1.62308000	2.36849000
F	0.15208200	1.62308000	-2.36849000
F	0.52977800	2.93731800	0.00000000
O	2.00375300	-2.67238500	0.00000000
H	1.46504500	-3.47323100	0.00000000
H	2.91587100	-2.98591000	0.00000000

Source – Reference [109]

Table 19 – Cartesian coordinates for $C_2F_4 \cdots$ TMA.

Atom	x	y	z
C	-1.801931	-0.291177	0.000000
C	-1.085165	0.834930	-0.000001
F	-0.716791	1.460715	-1.113179
F	-0.716787	1.460714	1.113177
F	-2.179558	-0.920645	1.113934
F	-2.179562	-0.920644	-1.113933
N	1.686389	-0.189331	-0.000001
C	2.756812	0.804237	-0.000015
H	2.668986	1.441161	-0.892555
H	2.668987	1.441183	0.892510
H	3.766540	0.335983	-0.000010
C	1.772906	-1.021558	-1.196933
H	0.948332	-1.750760	-1.202146
H	1.684252	-0.390221	-2.093412
H	2.733341	-1.580918	-1.253650
C	1.772908	-1.021528	1.196950
H	1.684256	-0.390169	2.093414
H	0.948335	-1.750731	1.202183
H	2.733344	-1.580887	1.253679

Source – Reference [113]

Table 20 – Cartesian coordinates for $\pi-$bonded $C_2F_3Cl \cdots$ TMA.

Atom	x	y	z
C	0.723806	0.995773	-0.450233
C	1.535134	0.225429	0.288012
F	1.769890	0.538744	1.581018
F	0.156211	2.102555	0.014249
F	0.449127	0.767019	-1.727473
Cl	2.276733	-1.210807	-0.269392
N	-1.845187	-0.291088	0.084319
C	-1.926261	-1.477360	-0.764452
H	-2.030983	-1.172765	-1.816220
H	-1.002938	-2.067658	-0.663656
H	-2.789410	-2.127472	-0.497978
C	-1.676040	-0.685631	1.480489
H	-0.757174	-1.282166	1.588635
H	-1.584398	0.211515	2.110895
H	-2.531047	-1.292362	1.853552
C	-3.051579	0.518688	-0.065762
H	-2.971295	1.419878	0.559845
H	-3.158136	0.831392	-1.115017
H	-3.970171	-0.035289	0.230912

Source – Reference [113]

Table 21 – Cartesian coordinates for $\pi-$bonded $C_2F_3Br\cdots TMA$.

Atom	x	y	z
C	0.092482	1.225808	-0.517521
C	1.006428	0.713604	0.319356
F	1.108138	1.206880	1.576026
F	-0.704157	2.237191	-0.191199
F	-0.076426	0.820671	-1.769225
Br	2.131492	-0.705412	-0.089668
N	-2.196447	-0.481178	0.096640
C	-2.065481	-1.724554	-0.658965
H	-2.212303	-1.523120	-1.730364
H	-1.055277	-2.137695	-0.518026
H	-2.806360	-2.491305	-0.339564
C	-1.971835	-0.733258	1.517759
H	-0.964703	-1.152553	1.665177
H	-2.040334	0.211663	2.077402
H	-2.712450	-1.447857	1.941149
C	-3.523294	0.094537	-0.107422
H	-3.604209	1.040932	0.447332
H	-3.674550	0.303648	-1.176771
H	-4.334695	-0.585548	0.235928

Source – Reference [113]

Table 22 – Cartesian coordinates for $\sigma-$bonded $C_2F_3Cl\cdots TMA$.

Atom	x	y	z
C	1.848688	0.565730	-0.006706
C	2.712265	-0.460391	0.000331
F	2.345620	-1.739207	-0.001384
F	4.034905	-0.309281	0.009960
F	2.327646	1.829414	-0.004058
Cl	0.146026	0.411278	-0.019041
N	-2.797640	-0.039468	-0.004405
C	-3.674754	1.087346	-0.312929
H	-3.514229	1.892228	0.419360
H	-3.439420	1.475600	-1.314797
H	-4.749924	0.801211	-0.290574
C	-3.081072	-0.544440	1.336882
H	-2.399126	-1.375551	1.570576
H	-2.920703	0.255476	2.074764
H	-4.127424	-0.909884	1.435906
C	-2.980942	-1.103274	-0.988860
H	-2.745993	-0.721860	-1.993558
H	-2.298199	-1.936292	-0.764370
H	-4.022598	-1.494526	-0.995753

Source – Reference [113]

Table 23 – Cartesian coordinates for $\sigma-$bonded $C_2F_3Br\cdots TMA$.

Atom	x	y	z
C	-1.871658	0.493138	0.000004
C	-2.793545	-0.481349	-0.000003
F	-2.504214	-1.780915	0.000006
F	-4.107730	-0.260063	-0.000019
F	-2.295355	1.781855	-0.000006
Br	-0.023389	0.229736	0.000026
N	2.804891	-0.122529	0.000003
C	3.188330	-0.869845	-1.197024
H	2.688752	-1.849801	-1.195701
H	2.871020	-0.317593	-2.093777
H	4.286654	-1.033285	-1.252866
C	3.189517	-0.861142	1.202040
H	2.873085	-0.302403	2.095078
H	2.689949	-1.841084	1.208316
H	4.287897	-1.024170	1.257984
C	3.433423	1.197823	-0.005096
H	3.116095	1.753779	-0.899574
H	3.116972	1.760257	0.885634
H	4.543246	1.131600	-0.005400

Source – Reference [113]

APPENDIX B – Published papers

Two papers were published with the results of this thesis, the first one reporting the method, early calibration of the probe and analysis of the Frustrated Lewis Pair, titled "Probing molecular environments with a fictitious isotopic dipole" [79], and one reporting the analysis of the compounds containing π- and σ-hole interactions, titled "Probing internal electric fields of π- and σ-hole bonds" [114]. Both papers were published in the International Journal of Quantum Chemistry, in 2019.